AGU PUBLICATIONS

Water Resources Research

RESEARCH ARTICLE
10.1002/2017WR021859

Special Section:
Dynamics in Intensively Managed Landscapes: Water, Sediment, Nutrient, Carbon, and Ecohydrology

Contextualizing Wetlands Within a River Network to Assess Nitrate Removal and Inform Watershed Management

Jonathan A. Czuba[1], Amy T. Hansen[2], Efi Foufoula-Georgiou[3], and Jacques C. Finlay[4]

[1]Department of Biological Systems Engineering, Virginia Tech, Blacksburg, VA, USA, [2]St. Anthony Falls Laboratory, University of Minnesota, Twin Cities, Minneapolis, MN, USA, [3]Department of Civil and Environmental Engineering, University of California, Irvine, CA, USA, [4]Department of Ecology, Evolution, and Behavior, University of Minnesota, Twin Cities, Minneapolis, MN, USA

Key Points:
- We present a framework for quantifying dynamic and spatially explicit nitrate removal and limiting factors in a wetland-river network
- Nitrate removal via denitrification can be limited by either nitrate, organic carbon, or residence time depending on flow conditions
- Spatial context of wetlands matters as nonlinearities from resource limitations lead to unexpected changes in downstream biogeochemistry

Correspondence to:
J. A. Czuba,
jczuba@vt.edu

Citation:
Czuba, J. A., Hansen, A. T., Foufoula-Georgiou, E., & Finlay, J. C. (2018). Contextualizing wetlands within a river network to assess nitrate removal and inform watershed management. *Water Resources Research*, *54*. https://doi.org/10.1002/2017WR021859

Received 15 SEP 2017
Accepted 1 FEB 2018
Accepted article online 9 FEB 2018

Abstract Aquatic nitrate removal depends on interactions throughout an interconnected network of lakes, wetlands, and river channels. Herein, we present a network-based model that quantifies nitrate-nitrogen and organic carbon concentrations through a wetland-river network and estimates nitrate export from the watershed. This model dynamically accounts for multiple competing limitations on nitrate removal, explicitly incorporates wetlands in the network, and captures hierarchical network effects and spatial interactions. We apply the model to the Le Sueur Basin, a data-rich 2,880 km^2 agricultural landscape in southern Minnesota and validate the model using synoptic field measurements during June for years 2013–2015. Using the model, we show that the overall limits to nitrate removal rate via denitrification shift between nitrate concentration, organic carbon availability, and residence time depending on discharge, characteristics of the waterbody, and location in the network. Our model results show that the spatial context of wetland restorations is an important but often overlooked factor because nonlinearities in the system, e.g., deriving from switching of resource limitation on denitrification rate, can lead to unexpected changes in downstream biogeochemistry. Our results demonstrate that reduction of watershed-scale nitrate concentrations and downstream loads in the Le Sueur Basin can be most effectively achieved by increasing water residence time (by slowing the flow) rather than by increasing organic carbon concentrations (which may limit denitrification). This framework can be used toward assessing where and how to restore wetlands for reducing nitrate concentrations and loads from agricultural watersheds.

1. Introduction

In pursuit of high crop yields, anthropogenic nitrogen inputs to agroecosystems have increased tenfold in the past 150 years (Galloway et al., 2008) and almost fivefold in the last half-century (Battye et al., 2017). In agricultural watersheds of the Midwestern U.S., an estimated 25% of applied nitrogen is flushed out of fields and into receiving surface waters in the form of nitrate-nitrogen (NO_3^-; referred to herein as nitrate) degrading local and downstream water quality (Donner & Scavia, 2007; Howarth et al., 2012; Keeler et al., 2016; Turner et al., 2008). For example, the water in tributaries of the Mississippi River regularly has nitrate concentrations that are too high for human consumption (Dubrovsky, 2010) and often the water-quality standards for supporting aquatic life are exceeded. Farther downstream, the size of the hypoxic zone in the northern Gulf of Mexico directly relates to the spring nitrate fluxes delivered from the Mississippi River Basin (Donner & Scavia, 2007; Turner et al., 2008). The pervasiveness of anthropogenic alterations of terrestrial nitrogen cycling and its downstream water-quality impacts has made this one of the most important global environmental issues we face today (Galloway et al., 2008; Rockström et al., 2009) and one of the grand challenges of this century (Perry et al., 2008).

Reducing nitrate in surface waters is imperative for maintaining healthy ecosystems while achieving prosperous and sustainable agroecosystems. Nitrate can be permanently removed from surface water via denitrification, a ubiquitous microbial oxidation-reduction process in which nitrogen is converted from nitrate to nitrogen gas (e.g., Knowles, 1982). Denitrification rate depends on the temperature and concentration of nitrate, organic carbon, and dissolved oxygen (Alexander et al., 2009; Bernot et al., 2006; Knowles, 1982; Seitzinger, 1988; Seitzinger et al., 2006). Both denitrification rate and water residence time affect the mass of nitrate that is removed from a surface waterbody and both can vary considerably across surface

waterbodies (Seitzinger et al., 2006; Tank et al., 2008; Wollheim et al., 2014). Wetlands often support high rates of denitrification and have long residence times compared to streams, which facilitates substantial nitrate removal (Baron et al., 2013; Jordan et al., 2011; Kadlec, 2012). Variations in denitrification rates and residence times contribute to wide variations in nitrate removal efficiencies (ranging from 1 to 99%) among individual wetlands, across wetland types, and across hydrologic conditions (Johnston, 1991; Jordan et al., 2011; Kovacic et al., 2000).

The net watershed-scale effect of a wetland complex to reduce nitrate through denitrification has been quantified often in very simple ways that ignore competing limiting factors arising from the dynamic connectivity of wetlands with the river network. For example, some studies have linearly upscaled nitrate removal rates for individual wetlands using hydraulic loading rates but have not taken into account the variability in denitrification rate with organic carbon availability or the dynamics that arise from the hierarchical spatial arrangement of wetlands (Crumpton, 2001; Crumpton et al., 2006; Mitsch et al., 2005). At the network scale, there have been a range of approaches to try to understand nitrogen dynamics—those range from data-driven empirical methods (such as the SPARROW model; Alexander et al., 2000; Smith et al., 1997) to multiparameter process-based modeling (e.g., Botter et al., 2006; Donner et al., 2002) and many approaches in between (Alexander et al., 2009; Helton et al., 2011, 2017; Seitzinger et al., 2002; Wollheim et al., 2006, 2008a, 2008b). However, these approaches consider only the river network and do not explicitly incorporate wetlands, which due to their connectivity to the river network change the system biogeochemistry spatially and over time.

The cumulative effect of the entire interconnected aquatic system (river reaches and wetlands) determines the downstream export of nitrate lost from the landscape. Recent research in the Le Sueur Basin, a 2,880 km^2 basin in the upper Midwest and our study area, has shown limited predictive ability for nitrate concentration at the outlet of a basin as a function of the percentage of wetlands alone (Hansen et al., 2018). This highlights the importance of explicitly considering wetland location and wetland characteristics, including the concentration of dissolved organic carbon (DOC), as part of the watershed-scale system dynamics. Overall, there is agreement in the literature that restoring wetlands within a small fraction of the landscape has the potential to significantly reduce nitrate export (Crumpton et al., 2006; Hansen et al., 2018; Mitsch et al., 2005). What is not known however is what is the optimal configuration of a set of wetlands in a watershed to maximize nitrate removal with the minimum amount of agricultural lands taken out of production? Moreover, in many watersheds, existing wetlands are largely relics of glacial and land use history and are not necessarily located in optimal positions for most effective nitrate removal. Given that biogeochemical processes are orchestrated by the movement of water and resources through networks of river channels and wetlands, effective management actions depend on understanding the collective biogeochemical functioning of these networks as affecting nitrate removal at the watershed scale.

Herein, we present a network-based model that quantifies nitrate-nitrogen and organic carbon concentrations through a wetland-river network and estimates nitrate export from the watershed. This model accounts for landscape configuration and individual wetland processing rates by explicitly considering controls on denitrification as nitrate and organic carbon are dynamically routed though the network. We apply the model to the Le Sueur Basin, a 2,880 km^2 agricultural landscape in southern Minnesota, and validate the model using synoptic field measurements during June (a critical period for nitrate transport) for years 2013–2015. Using the model, we show how interactive effects of wetlands within a river network influence the space-time dynamics of nitrate concentration. Our ultimate goal is to develop a framework for assessing where and with what specifications to restore wetlands for optimal environmental benefits in a watershed.

2. Model Formulation

We present a watershed-scale, network-based model that quantifies nitrate concentrations through a dynamically interacting wetland-river connected network. The developed model is applicable to watersheds within temperate agricultural landscapes (such as in the agricultural Midwestern U.S. Corn Belt) during spring (April–June) when denitrification is the primary nitrate removal process. Developing the model in this way simplifies the biogeochemical dynamics yet captures important processes under spring conditions when most of the annual aquatic nitrate load is delivered to the northern Gulf of Mexico (Goolsby et al., 2000; Hubbard et al., 2011; Kalkhoff et al., 2016; Royer et al., 2006; Schilling et al., 2012). The following

processes/factors were excluded from the model: (1) in-stream nitrate generation (i.e., nitrification), because agricultural watersheds with high synthetic fertilizer use typically have low ammonium concentrations and nitrate supplied by in situ nitrification is relatively low compared to other sources (Birgand et al., 2007; Duff et al., 2008); (2) temperature variations, because this was shown to be less variable, limiting, and responsive to network structure than nitrate and organic carbon during April–June (Hansen et al., 2016); and (3) nitrate assimilation, because this is minimal during spring to early summer within the region (Kreiling et al., 2010). Additionally, we assume that anoxic conditions can be found within the sediment throughout the benthic area although the depth may vary, and that bulk water concentrations of nitrate and dissolved organic carbon are a reasonable proxy for concentrations near the surface of denitrifying microbial organisms.

The model also quantifies dissolved organic carbon concentrations because the supply of organic carbon can be low in agricultural landscapes and thus limit denitrification (Bernhardt & Likens, 2002; Hansen et al., 2016; Inwood et al., 2007; Zarnetske et al., 2011). Although particulate organic carbon is potentially available for denitrification (Arango et al., 2007), we only model dissolved organic carbon because it is likely more accessible to microbes, widely distributed throughout all locations and microhabitats, and thus likely to be the most important form for watershed-scale denitrification (e.g., Findlay & Sinsabaugh, 2003; Stelzer et al., 2015). Hereafter, the term organic carbon refers to the dissolved fraction.

We map a watershed into a network of surface-water flow paths conceptualized as a set of connected links (Figure 1a) following the framework developed by Czuba and Foufoula-Georgiou (2014, 2015). A link i represents a segment of river channel or a wetland that is directly connected to the river network each with a set of unique topologic, hydrodynamic, and biogeochemical attributes. The term wetland is used herein to represent all lentic waterbodies including lakes. Isolated wetlands, while important landscape elements (Cohen et al., 2016; Golden et al., 2017), are not as dynamically connected to the river network as are flow-through wetlands, and thus affected only the inputs to the network in the present model.

We develop below the framework accounting for nitrate concentration N_i [$M\,L^{-3}$; where M is a unit of mass and L is a unit of length] and organic carbon concentration C_i [$M\,L^{-3}$] over the entire wetland-river connectivity network. For every connected waterbody (channel or wetland) i we can write the following conservation equations.

For channels:

$$N_{out,i} = N_{in,i} - \frac{J_{den,i}(N_i, C_i)\mathcal{A}_{c,i}}{Q_i} \tag{1}$$

$$C_{out,i} = C_{in,i} - \frac{J_{den,i}(N_i, C_i)\mathcal{A}_{c,i}}{Q_i} \tag{2}$$

For wetlands:

$$N_{out,i} = N_{in,i} - \frac{J_{den,i}(N_i, C_i)\mathcal{A}_{w,i}}{Q_i} \tag{3}$$

$$C_{out,i} = C_{in,i} - \frac{J_{den,i}(N_i, C_i)\mathcal{A}_{w,i}}{Q_i} + \frac{J_{prod}\mathcal{A}_{vw,i}}{Q_i} \tag{4}$$

where $N_{out,i}$ and $N_{in,i}$ [$M\,L^{-3}$] is the nitrate concentration out of and into, respectively, link i, $C_{out,i}$ and $C_{in,i}$ [$M\,L^{-3}$] is the dissolved organic carbon concentration out of and into, respectively, link i, Q_i [$L^3\,T^{-1}$; where T is a unit of time] is the flow discharge through link i, $\mathcal{A}_{c,i}$ [L^2] is the wetted area in channel link i where denitrification takes place approximated here as the bed surface area:

$$\mathcal{A}_{c,i} \cong \ell_i B_i \tag{5}$$

where ℓ_i [L] is the channel link length and B_i [L] is the average channel width, $\mathcal{A}_{w,i}$ [L^2] is the wetted area in wetland link i where denitrification takes place approximated here as the wetland surface area $W_{A,i}$ [L^2], i.e.,

$$\mathcal{A}_{w,i} \cong W_{A,i} \tag{6}$$

$\mathcal{A}_{vw,i}$ [L^2] is the areal extent of emergent vegetation in wetland link i approximated here as

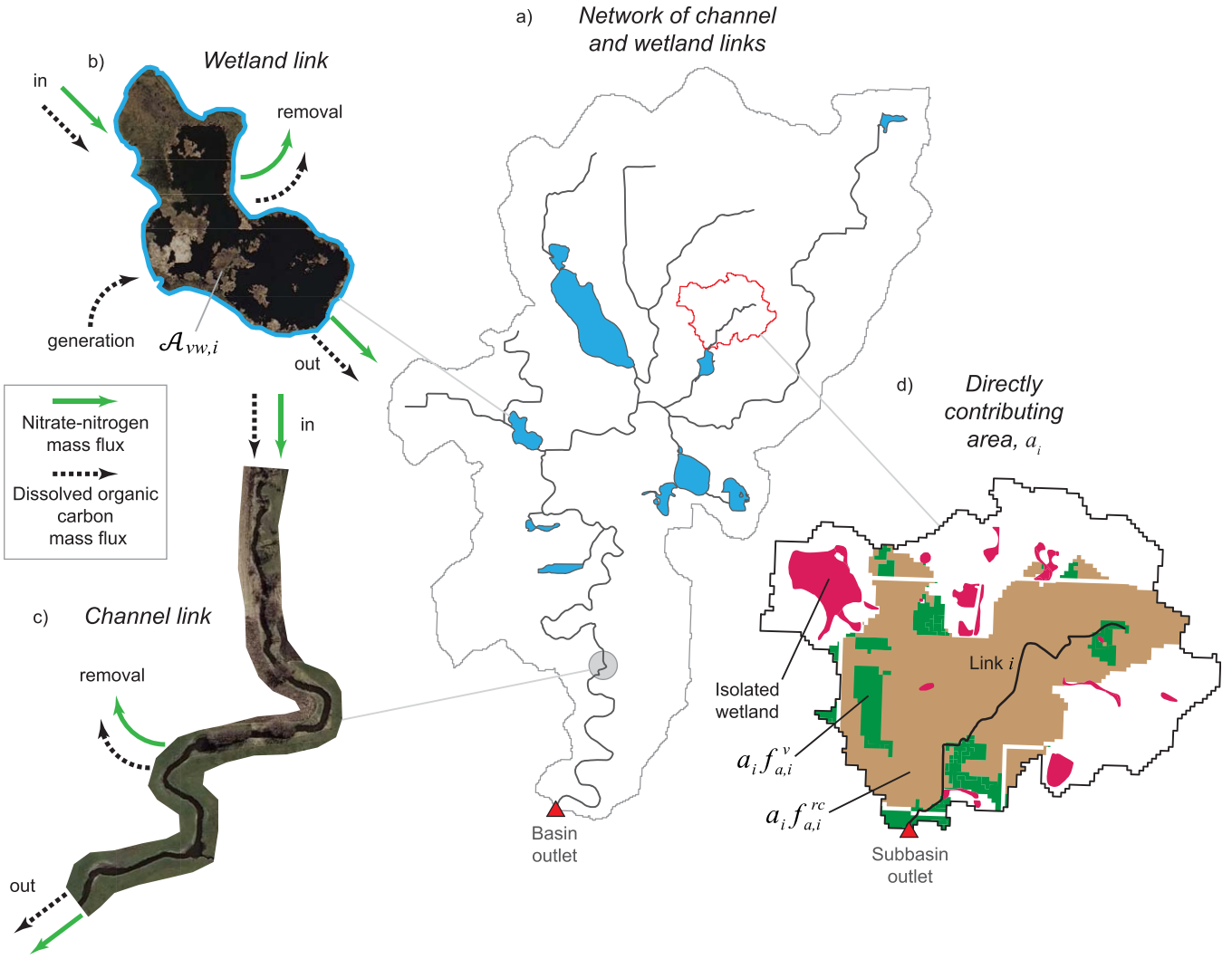

Figure 1. Conceptual overview of the model. (a) Decomposition of a watershed into a connected set of links representing channels and wetlands. Conservation of nitrate (green arrows) and dissolved organic carbon (black arrows) within a (b) wetland and (c) channel link. Note that within a wetland, our model generates dissolved organic carbon from the wetland area with emergent vegetation $\mathcal{A}_{vw,i}$ thereby affecting $C_i : N_i$ and thus denitrification. (d) The directly contributing area a_i to link i; $f^{rc}_{a,i}$ is the fraction of the directly contributing area that is row-crop agriculture and not intercepted by isolated wetlands—only this fraction generates nitrate to the network, $f^{v}_{a,i}$ is the fraction of the directly contributing area that is vegetated without row crops (which also excludes barren and developed lands) and not intercepted by isolated wetlands.

$$\mathcal{A}_{vw,i} \cong W_{A,i} f_{em,i} \tag{7}$$

where $f_{em,i}$ is the fraction of emergent vegetation in wetland link i, $J_{den,i}(N_i, C_i)$ $[M\,L^{-2}\,T^{-1}]$ is the denitrification flux in link i with functional dependence on both the nitrate concentration N_i and organic carbon concentration C_i, i.e.,

$$J_{den,i} = f(N_i, C_i) \tag{8}$$

where the form of $f(N_i, C_i)$ needs to be specified, and J_{prod} $[M\,L^{-2}\,T^{-1}]$ is a vegetation organic carbon production flux. Implicit in equations (1)–(4) is the time scale over which the processes take place, which is variable for each link and represents the travel time through the link. This formulation further assumes that the mass of nitrate or organic carbon is completely mixed within the waterbody (i.e., within each link i). We recognize that this assumption will not be satisfied everywhere, but is a necessary simplifying assumption in the absence of higher fidelity parameterizations suitable for hundreds of wetlands within a basin.

Denitrification flux rates $J_{den,i}$ in waterbodies within agricultural watersheds of the Midwestern U.S. during April–June are typically limited by nitrate or organic carbon (Bernhardt & Likens, 2002; Hansen et al., 2016; Inwood et al., 2007; Zarnetske et al., 2011). The threshold is set by the ratio of organic carbon concentration to nitrate concentration, given as $C_i : N_i$. Specifically, the denitrification flux rate $J_{den,i}$ is considered nitrate limited where $C_i : N_i > 1$, and organic carbon limited where $C_i : N_i < 1$ (Stubbins, 2016; Taylor & Townsend, 2010). Under nitrate-limited conditions, it is common to parameterize the denitrification flux rate as a function of nitrate concentration (Bohlke et al., 2009; Hansen et al., 2016; Mulholland et al., 2008). Without a similar parameterization established for the denitrification flux rate under carbon-limited conditions, we assumed here a parameterization as a function of organic carbon concentration. Thus, the denitrification flux rate can be expressed as

$$J_{den,i} = \begin{cases} f(N_i), \text{ for } C_i : N_i \geq 1 \\ f(C_i), \text{ for } C_i : N_i < 1 \end{cases} \tag{9}$$

where both functions $f(\cdot)$ are derived based on observations via data fitting and/or calibration.

The removal term (representing denitrification) in equations (1)–(4) has the same form for both nitrate and organic carbon because both are utilized equally during denitrification (Knowles, 1982; Taylor & Townsend, 2010). The only generation term (in equation (4)) represents the production of dissolved organic carbon by aquatic vegetation via leaching and microbial processes. We assumed that this term was nonzero only for wetlands, which have been shown to be an important source of organic carbon, and at the watershed scale are often predictive of in-stream organic carbon (Gergel et al., 1999; Gorham et al., 1998; Hansen et al., 2018; Wilson & Xenopoulos, 2008; Wollheim et al., 2015). Dissolved organic carbon production by phytoplankton and benthic algae was assumed to be negligible compared to abundant emergent vegetation during springtime for which the model is formulated.

Inputs to a link were supplied by the directly contributing area a_i [L^2] and from the directly upstream links. Because the model was formulated in terms of concentration (equations (1)–(4), the mass that was input to a link must be renormalized into a concentration relevant to the receiving link (under the assumption of complete mixing). The nitrate concentration into a link $N_{in,i}$ is the flow-weighted concentration from a link's directly contributing area and from upstream tributaries as

$$N_{in,i} = \frac{N_{out,j}Q_j + N_{out,k}Q_k + N_{a,i}Q_{a,i}}{Q_i} \tag{10}$$

where indices j and k denote directly upstream links and the subscript "a,i" denotes contributions from the directly contributing area to link i. Similarly, the dissolved organic carbon concentration into a link $C_{in,i}$ is given as

$$C_{in,i} = \frac{C_{out,j}Q_j + C_{out,k}Q_k + C_{a,i}Q_{a,i}}{Q_i} \tag{11}$$

The values $N_{a,i}$ and $C_{a,i}$ represent known inputs from the landscape that can be specified for each link in the model. For nitrate, at each link i we sum over all land use classes within a_i, i.e., as

$$N_{a,i} = \sum_{\substack{land-use \\ class \\ m}} N_{nom}^m f_{a,i}^m \tag{12}$$

where N_{nom}^m [$M\,L^{-3}$] is the nominal nitrate concentration input from land-use m and $f_{a,i}^m$ is the fraction of the directly contributing area a_i classified as land-use m that drains to link i without being intercepted by isolated wetlands. Similarly for organic carbon:

$$C_{a,i} = \sum_{\substack{land-use \\ class \\ m}} C_{nom}^m f_{a,i}^m \tag{13}$$

where C_{nom}^m [$M\,L^{-3}$] is the nominal organic carbon concentration input from land-use m.

In our model, the mass of nitrate removed in any given link depends on the denitrification rate (i.e., controlled by resource availability via $C_i : N_i$ as discussed previously, and hereafter referred to as resource limitation) and on nitrate residence time (due to flow rate) within that link. This interplay between resource

availability and residence time can be conveniently expressed as the Damköhler number Da_i. The Damköhler number is the ratio of the convective mass transport time scale $\tau_{trans,i}$ [T] (residence time) to the biogeochemical reaction (denitrification) time scale $\tau_{react,i}$ [T] (Pinay et al., 2015) as

$$Da_i = \frac{\tau_{trans,i}}{\tau_{react,i}} \tag{14}$$

Whichever time scale is shorter limits nitrate removal (see Appendix A for the specific calculation of the Damköhler number). Thus, if $Da_i < 1$, residence time limits nitrate removal regardless of $C_i : N_i$. If $Da_i > 1$, resource supply limits nitrate removal and we next need to look at $C_i : N_i$ to determine if the overall limitation on nitrate removal is due to nitrate concentration ($C_i : N_i > 1$) or organic carbon concentration ($C_i : N_i < 1$).

3. Application to the Le Sueur Basin

We applied the model to the 2,880 km^2 Le Sueur Basin (Figure 2) where 82% of land use is agriculture (Homer et al., 2015), predominantly corn and soybeans. Most precipitation falls in the springtime, becomes quickly conveyed through agricultural tile drains rather than persisting as groundwater, and thus contributes to high streamflows (Foufoula-Georgiou et al., 2015). The Le Sueur Basin is one of the largest contributors of nitrate within the state of Minnesota (Minnesota Pollution Control Agency [MPCA], 2013) and annual nitrate yields here are among the highest in the Mississippi River Basin (Robertson & Saad, 2014). Thus, improved understanding of nitrate dynamics within and delivery from this basin can inform effective management strategies for reducing nitrate, even from the largest contributors, in agricultural landscapes.

The river network was obtained from the National Hydrography Dataset Plus Version 2 (NHDPlusV2; Horizon Systems, 2014; McKay et al., 2012). Wetlands were obtained from the National Wetlands Inventory update

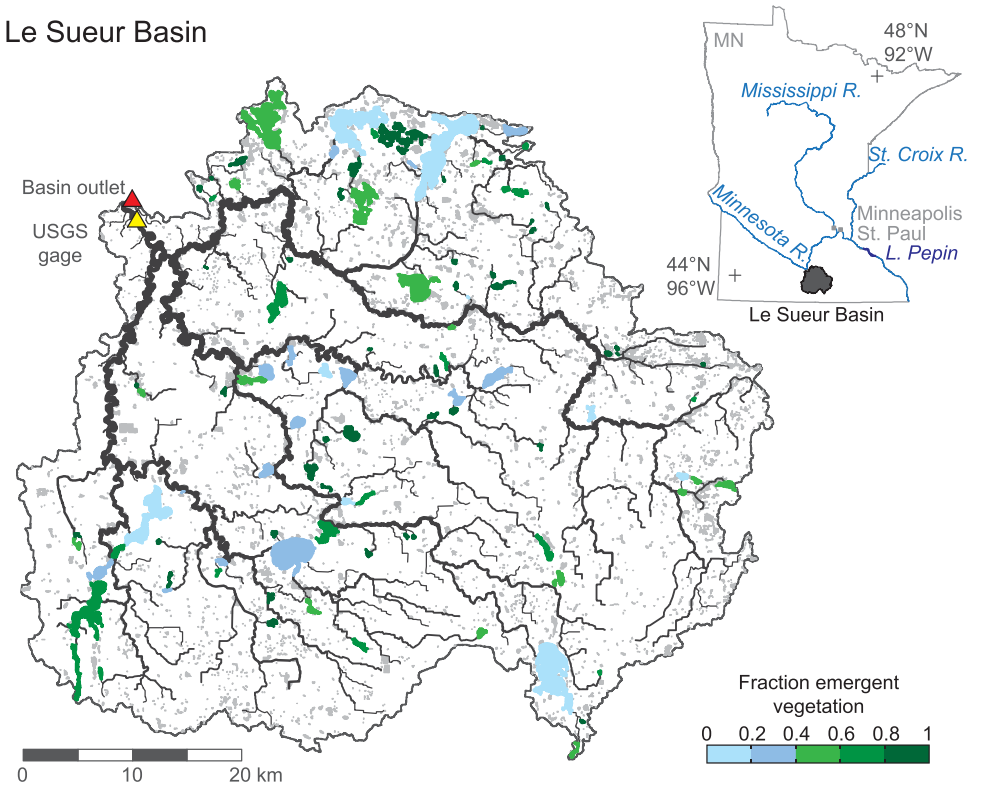

Figure 2. Wetland-river network in the Le Sueur Basin. Shown is the channel network (dark gray; thicker lines correspond to reaches with larger upstream drainage areas), connected wetlands (incorporated into the model as individual links) colored according to fraction emergent vegetation $f_{em,i}$, and isolated wetlands (light gray). Inset shows a location map of the Le Sueur Basin relative to the state of Minnesota.

for Minnesota, which was based on 2011 spring aerial imagery (Minnesota Department of Natural Resources, 2015). Wetlands were first classified as either (a) connected, flow-through or (b) isolated depending on whether they intersected the NHDPlusV2 network or had a visible, channelized connection to the network in the 2011 aerial imagery. The NHDPlusV2 network was clipped to the extent of the Le Sueur Basin, isolated and secondary channels were removed as well as channels not associated with actual channels visible in the 2011 aerial imagery, and a few short links were added to connect wetlands directly to the network where they had a visible connection to the network in the 2011 aerial imagery but without a respective channel in the NHDPlusV2 network. Links were then established (assigned a unique index i) for every connected wetland and for segments of river channel either between tributary junctions or no longer than 5 km. The final network was composed of 643 links including 540 channel and 103 wetland links.

The directly contributing area a_i to each link was computed from the digital elevation model associated with the NHDPlusV2 network. The upstream drainage area A_i [L^2] was calculated as the sum of a_i for all links upstream of and including link i. Link length ℓ_i was directly computed from the channel link geometry. Relevant wetland attributes associated with the source data included surface area $W_{A,i}$ and fraction covered by emergent vegetation $f_{em,i}$, according to the classification system developed by Cowardin et al. (1979).

Flow discharge for the entire network was scaled from the daily flow at the USGS streamflow-gaging station near the basin outlet (Le Sueur River near Rapidan, MN, 05320500; U.S. Geological Survey [USGS], 2016). The flow for each link, Q_i was scaled based on upstream drainage area A_i as

$$Q_i = \left(\frac{Q_{gage}}{A_{gage}}\right) A_i \tag{15}$$

This assumes a scaling exponent of one (Rodriguez-Iturbe & Rinaldo, 1997), which is known to vary (e.g., Ayalew et al., 2015), but we tested this assumption against field measurements of flow discharge throughout the basin (see section 4). Similarly, the width for channel links throughout the network was scaled from the channel width at the gage following downstream hydraulic geometry relationships. The channel width at the gage for a given flow $B_{gage} = f\left(Q_{gage}\right)$ [L] was first determined from a rating curve fit to field measurements of flow versus channel width. Then the channel width throughout the basin B_i was scaled based on upstream drainage area assuming a typical exponent of 0.5 (Leopold & Maddock, 1953; Park, 1977) as

$$B_i = \left(\frac{B_{gage}}{A_{gage}^{0.5}}\right) A_i^{0.5} \tag{16}$$

As this scaling relation was also assumed, we tested this assumption against field measurements of channel width throughout the basin (again, see section 4).

We assumed all terrestrial nitrate inputs originated from row-crop agriculture. Thus, for equation (12), when row-crop agriculture is the only relevant land use, the terrestrial nitrate input $N_{a,i}$ becomes

$$N_{a,i} = N_{nom}^{rc} f_{a,i}^{rc} \tag{17}$$

where the superscript rc denotes the row-crop agricultural land use class. In addition to the organic carbon generated internally by connected wetlands, we accounted for distinct terrestrial organic carbon inputs from row-crop agricultural lands and nonagricultural, vegetated lands (see Figure 1d). Thus, for equation (13), the terrestrial organic carbon input $C_{a,i}$ becomes

$$C_{a,i} = C_{nom}^{rc} f_{a,i}^{rc} + C_{nom}^{v} f_{a,i}^{v} \tag{18}$$

where the superscript v denotes the nonagricultural, vegetated land use class. The fraction of the directly contributing area that is not intercepted by isolated wetlands and is either (1) row-crop agriculture $f_{a,i}^{rc}$ or (2) vegetated without row crops and excluding barren and developed lands $f_{a,i}^{v}$ was computed from the 2011 national land-cover data set (Homer et al., 2015).

Nominal nitrate and organic carbon concentrations from row-crop agricultural lands, N_{nom}^{rc} and C_{nom}^{rc}, respectively, were constrained by observations of subsurface drainage tile effluent. These nominal concentrations were set at reasonable values near the upper limit of drainage tile effluent concentrations (because of outliers, at roughly the 85th percentile values) from field measurements (18 observations of nitrate concentration and 19 observations of organic carbon concentration in tile effluent during May–June of 2013–2015;

the 85th percentile is roughly the third largest value). Thus, N^{rc}_{nom} was set to 30 mg L^{-1} and C^{rc}_{nom} was set to 4.5 mg L^{-1} (Dolph et al., 2017a). Nitrate inputs from terrestrial sources can vary with antecedent moisture conditions which affect how much organic nitrogen in the soil is converted and mobilized (Davis et al., 2014). However, we do not capture these dynamics in the present model.

Within streams of the agricultural Le Sueur Basin, Hansen et al. (2016) showed that denitrification flux rates $J_{den,i}$ were either nitrate or organic carbon limited. For nitrate-limited conditions, they were able to fit an empirical relation to their data similar to that of Mulholland et al. (2008) and Bohlke et al. (2009). However, under conditions of relatively low organic carbon availability, Hansen et al. (2016) did not find a statistically significant relationship between DOC and denitrification rate. Lack of apparent influence of carbon limitation could arise from the small sample size and lack of information on the bioavailable pool of DOC (Fork & Heffernan, 2014; Grebliunas & Perry, 2016; Wilson & Xenopoulos, 2008; Zarnetske et al., 2011) or DOC levels that were just above limitation thresholds (Hansen et al., 2016). In the absence of an empirical relation for organic carbon-limited conditions, we assumed the simplest linear functional form and calibrated the parameter value. Thus, the denitrification flux rate $J_{den,i}$ under nitrate-limited conditions (Hansen et al., 2016) and organic carbon-limited conditions was specified as

$$J_{den,i} = \begin{cases} 11.5N_i^{0.5}, & \text{for } C_i : N_i \geq 1 \\ \lambda C_i, & \text{for } C_i : N_i < 1 \end{cases} \tag{19}$$

where λ is the parameter of the organic carbon-limited denitrification flux equation. Equation (19) is an empirical relation with concentration N_i and C_i specified in mg L^{-1} and $J_{den,i}$ in mg m^{-2} h^{-1}.

Three parameter values were poorly constrained: the nominal dissolved organic carbon concentration from nonagricultural, vegetated lands C^{v}_{nom}, the vegetation organic carbon production flux J_{prod}, and the parameter of the organic carbon-limited denitrification flux equation λ. These uncertain values were obtained through model calibration as discussed in section 4. Calibration ranges for these parameters were guided by previously reported net organic carbon flux, which ranged from 3 to 22 mg OC m^{-2} h^{-1} (Bertilsson & Jones, 2003; Butman et al., 2016; Dalzell et al., 2011; Juckers et al., 2013).

The computation of nitrate and organic carbon concentration for every link in the network proceeded as follows: (1) determine a flow at the gage and its associated channel width, then scale the flow discharge throughout the network (equation (15)) and width to all channel links (equation (16)); (2) assign nitrate and organic carbon concentrations input from each directly contributing area to its associated channel or wetland link (equations (17) and (18)); (3) determine, progressing downstream in a hierarchical fashion, the flow-weighted concentration of nitrate and organic carbon input to each link from upstream (equations (10) and (11)); and (4) compute the nitrate and organic carbon concentrations output from each link (equations (1)–(4)). During the computation for wetland links, organic carbon was first produced and added to the organic carbon inputs before determining the organic carbon to nitrate ratio, denitrification flux, and the subsequent reduction in nitrate concentration. Nitrate concentration N_i and organic carbon concentration C_i as reported in the model results refers to $N_{out,i}$ and $C_{out,i}$, respectively.

Results are presented for a range of flows, but we highlight model results at the 50% (low flow), 10%, and 1% (high flow) daily flow exceedance (i.e., probability that the flow on a given day will be equaled or exceeded). Daily flow exceedance was determined from daily flow discharge data at the USGS gaging station Le Sueur River near Rapidan, MN (05320500) between 1976 and 2015 (USGS, 2016); the time period characteristic of the present-day intensive agricultural drainage regime (Foufoula-Georgiou et al., 2015). The model provides a snapshot of system functioning at a given flow condition by highlighting spatial variations in nitrate concentrations resulting from the configuration and characteristics of the network and the underlying process dynamics for a given steady state flow condition.

4. Model Calibration, Validation, and Sensitivity

Model calibration and validation data included observations of flow discharge, channel width, nitrate concentration, and organic carbon concentration collected on 11–12 June 2013, 23–24 June 2014, and 15–16, 18 June 2015 throughout the network (Figure 3; Dolph et al., 2017a, 2017b). Channel width was observed at the same times and locations as flow discharge (Figures 3e–3g) except at the subset of sites shown in Figure

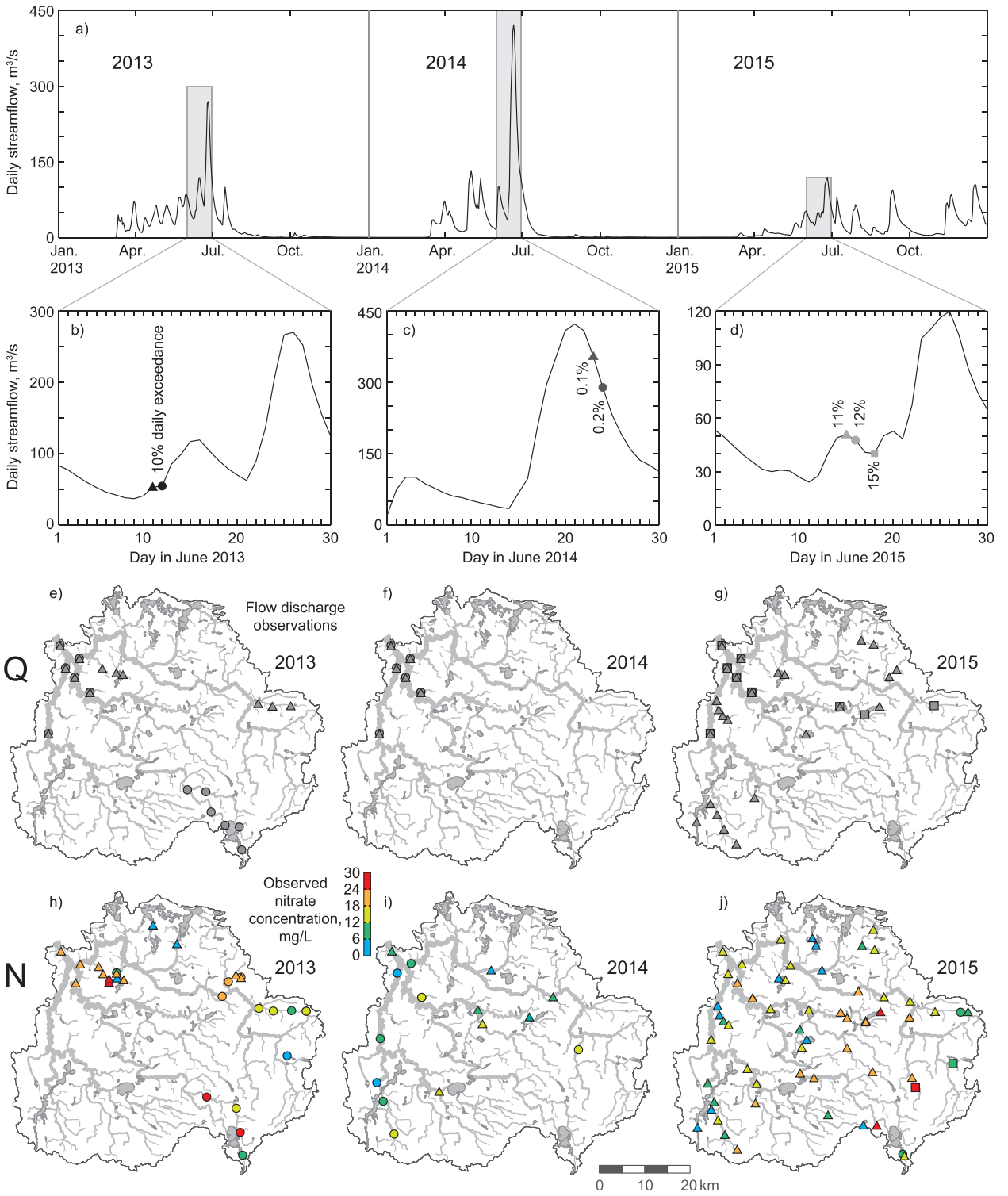

Figure 3. Observations used for model calibration and validation. (a) Daily streamflow data measured at the USGS gage (05320500) on the Le Sueur River near Rapidan, MN, over the period of field data collection: (b) 11–12 June 2013, (c) 23–24 June 2014, and (d) 15–16, 18 June 2015, with the probability of daily exceedance noted for the flow on each day of data collection. Spatial locations where flow discharge was measured in (e) 2013, (f) 2014, and (g) 2015 and where nitrate concentration was measured in (h) 2013, (i) 2014, and (j) 2015. Symbols in Figures 3e–3j correspond to specific days of data collection consistent with symbols in Figures 3b–3d, respectively.

3f for all dates. No calibration of flow discharge or channel width was performed, only validation. Organic carbon concentration was measured concurrently with nitrate (Figures 3h–3j). The observations of nitrate and organic carbon concentration were split at random into either a calibration or validation set. The model was run for each of these 7 days based on the daily discharge at the gage. Then the field observations were compared to the model results at the link nearest to each sampling site.

Model calibration involved setting C^v_{nom} in the range of 1–200 mg L^{-1} with increments of 10 mg L^{-1} (21 values), J_{prod} in the range of 1–100 mg m^{-2} h^{-1} with increments of 5 mg m^{-2} h^{-1} (21 values), and λ in the range of 0.1–10 with increments of 0.5 (21 values). A total of 9,261 (21^3) parameter combinations were simulated in the model at the seven daily discharges corresponding to field observations for a total of 64,827 model runs during calibration. For each parameter combination, we computed the root-mean-square error (RMSE) between predicted and observed values of nitrate concentration and also of organic carbon concentration.

The primary role of organic carbon concentration in the model is to compute $C_i : N_i$ to determine which resource limitation equation to use for $J_{den,i}$ (see equation (19)). Thus, it is more important to accurately classify whether $C_i : N_i > 1$ or $C_i : N_i < 1$ than it is to accurately predict the organic carbon concentration. Therefore, we compared the predicted classification of $C_i : N_i > 1$ or $C_i : N_i < 1$ versus the observed classification using a confusion matrix (e.g., Fawcett, 2006). From this matrix we computed the accuracy *ACC* and Matthews correlation coefficient *MCC* as

$$ACC = \frac{TP + TN}{TP + TN + FP + FN} \tag{20}$$

and

$$MCC = \frac{TP \times TN - FP \times FN}{\sqrt{(TP + FP)(TP + FN)(TN + FP)(TN + FN)}} \tag{21}$$

where *TP* is the number of true positives, *TN* is the number of true negatives, *FP* is the number of false positives, and *FN* is the number of false negatives (e.g., Fawcett, 2006; Powers, 2011). *ACC* is a value between 0 and 1 with a value of one representing a perfect prediction. *MCC* is a value between −1 and 1 where −1 characterizes complete disagreement, 0 characterizes a random prediction, and 1 characterizes a perfect prediction. Compared to *ACC*, *MCC* is a more balanced measure of agreement between binary classifications, particularly for classes of different sizes.

Once the model simulated all parameter combinations, the optimal values were chosen by first selecting the subset of parameter values at the maximum *MCC* (based on predicted versus observed values of $C_i : N_i$). Note that there were more than one set of parameter values at the maximum *MCC*. From this subset of parameter values, the optimal values were chosen by next selecting the parameter values at the minimum RMSE for organic carbon concentrations. The RMSE for nitrate concentrations was also computed, but this was not used in selecting the optimal parameter values. The calibrated values were: C^v_{nom} of 90 mg L^{-1}, J_{prod} of 85 mg m^{-2} h^{-1}, and λ of 3.5. The values for the *MCC* of $C_i : N_i$ and RMSE of nitrate and organic carbon concentrations throughout the calibration parameter space are shown in Figure 4. Note the relatively large range in *MCC* of $C_i : N_i$ (0.1–0.7) and RMSE of organic carbon concentrations (5–16 mg/L) compared to the RMSE of nitrate concentrations (4.8–6.7 mg/L). This demonstrates that the predicted nitrate concentrations were largely insensitive to these parameters for organic carbon for the existing conditions of the Le Sueur Basin.

Despite scaling flow discharge and channel width throughout the entire basin using assumed exponents of hydraulic geometry relations and coefficients determined from the gage near the outlet of the basin, the predicted values were fairly close to the observations (Figures 5a and 5b): an RMSE of 4.0 m^3 s^{-1} for flow discharge (76 observations, obs.) and an RMSE of 1 m for channel width (34 obs.). Note that channel width was only observed at small-scale sites (widths less than 10 m in Figure 5b), whereas the channel width at the USGS gage used for setting the coefficient of the hydraulic geometry relation was over 40 m.

Nitrate concentrations were reasonably well predicted by the model with an RMSE of 5.0 mg L^{-1} during calibration (54 obs.) and 5.6 mg L^{-1} during validation (48 obs.; Figure 5c). Organic carbon concentrations were less accurately predicted by the model with an RMSE of 8.3 mg L^{-1} during calibration (57 obs.) and 7.7

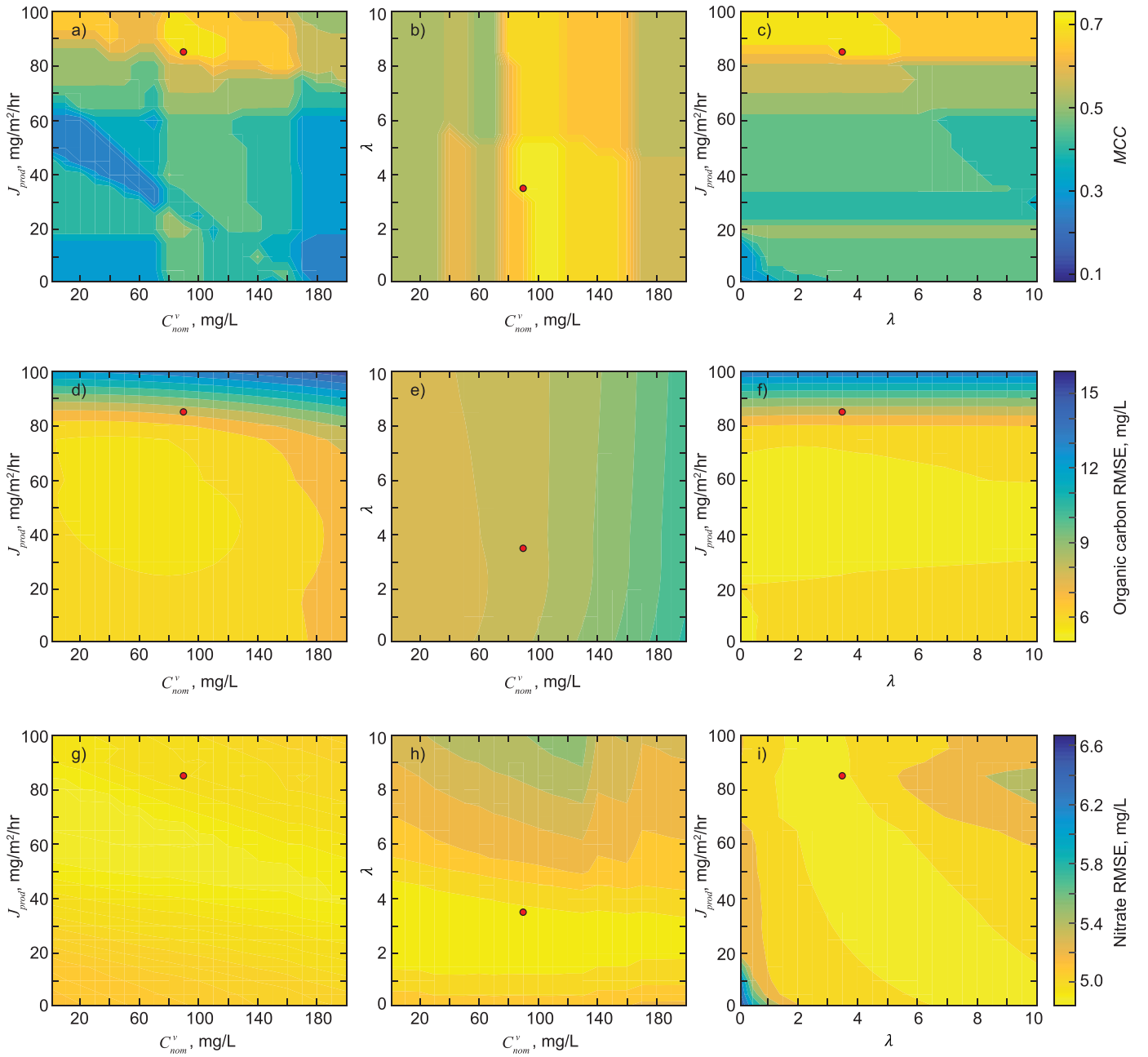

Figure 4. Model calibration space shown as three planes through the optimal parameter values (red dots). The calibrated parameters included: the nominal organic carbon concentration from nonagricultural, vegetated lands C^v_{nom}, the vegetation organic carbon production flux J_{prod}, and the parameter of the organic carbon-limited denitrification flux equation λ. (a–c) Contour is the Matthews correlation coefficient *MCC* for the classification of $C_i : N_i > 1$ or $C_i : N_i < 1$. Contour is the root-mean-square error (RMSE) between predicted and observed values of (d–f) organic carbon concentration and also of (g–i) nitrate concentration.

mg L^{-1} during validation (49 obs.; Figure 5d). However, $C_i : N_i$ was classified reasonably well with an *ACC* of 0.9 during calibration (53 obs.) and 0.85 during validation (47 obs.), and with an *MCC* of 0.73 during calibration (53 obs.) and 0.63 during validation (47 obs.; Figure 5e).

The most uncertain parameters in the model were the three calibration parameters (C^v_{nom}, J_{prod}, and λ) and the nominal nitrate and organic carbon concentrations from row-crop agricultural lands N^{rc}_{nom} and C^{rc}_{nom}, respectively. For these five parameters, we assessed the sensitivity of the model results by changing each parameter value individually by ±10%. The effect of changing each of these parameters is shown along with the model results.

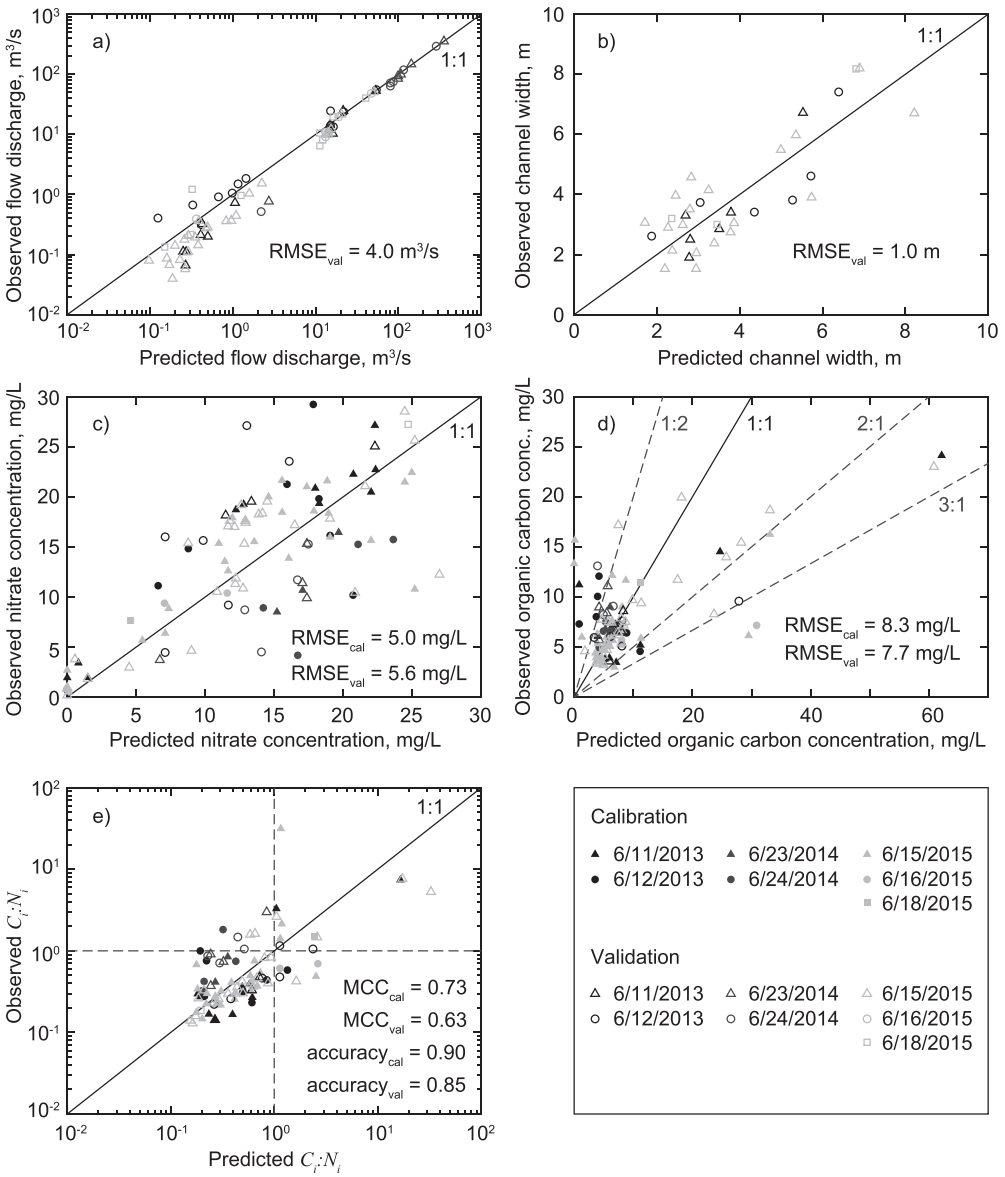

Figure 5. Comparison of predicted and observed values for model calibration and validation. Validation of (a) flow discharge and (b) channel width. Calibration and validation of (c) nitrate concentration, (d) organic carbon concentration, and (e) $C_i : N_i$ via the Matthews correlation coefficient *MCC*.

5. Results

5.1. General Model Behavior

The general behavior of the model for a river reach with and without an upstream wetland and in the absence of tributaries is shown in Figure 6. Concentration in a link was affected by three factors: (1) the mass supplied from directly contributing areas and generated internally (for organic carbon produced by wetlands), (2) the denitrification rate acting to remove mass from the system, and (3) dilution due to increasing flow progressing downstream. For a river reach without an upstream wetland (Figure 6, blue lines), simulated nitrate concentrations were high and organic carbon concentrations were low throughout the reach, which resulted in a low denitrification rate set by the limited supply of organic carbon.

When an upstream wetland was present (Figure 6, orange lines), simulated nitrate concentrations were low immediately downstream and increased as nitrate was added from downstream directly contributing areas. Conversely, simulated organic carbon concentrations were high immediately downstream of the wetland,

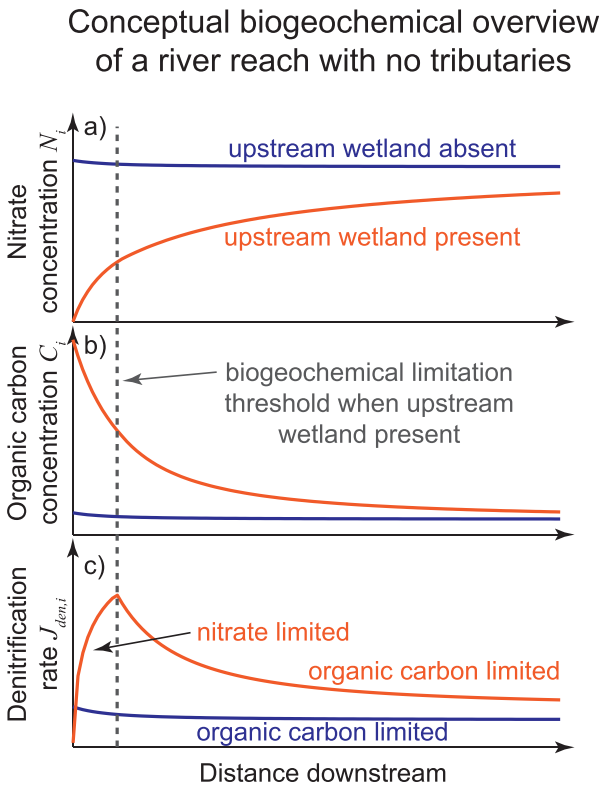

Figure 6. Overview of model behavior. General conditions of (a) nitrate concentration N_i, (b) organic carbon concentration C_i, and (c) denitrification rate $J_{den,i}$ for a river reach with no tributaries when an upstream wetland is present (orange) or absent (blue).

due to high rates of organic carbon production by wetland vegetation, and decreased downstream as organic carbon was consumed in the denitrification process as well as diluted with low organic carbon inputs from downstream directly contributing areas. These simulated dynamics resulted in a shift from nitrate-limited denitrification near the wetland outlet to organic carbon-limited denitrification farther downstream. Because the denitrification rate was directly related to nitrate concentration under nitrate-limited conditions and to organic carbon concentration under organic carbon-limited conditions (see equation (19)), simulated denitrification rates were highest at a location downstream of the wetland where the two resources were balanced. The distance between the wetland outlet and the local peak in denitrification rate will vary depending on wetland characteristics and location in the network.

When this model was applied to an existing network of wetlands and river channels, such as in the Le Sueur Basin (Figure 2), the model behavior became much more complex. Tributaries disrupted the gradual progression of simulated nitrate and organic carbon concentrations. Wetlands were interspersed with river channels thus leading to an integration of effects from individual features to downstream links. Spatial heterogeneity in the distribution of isolated wetlands created a spatial heterogeneity in inputs to waterbodies despite a relatively homogeneous row-crop agricultural landscape.

5.2. Network-Wide Results

Simulated nitrate concentrations varied spatially across the basin (Figures 7b and 7c). At low flow (Figure 7b), nitrate concentrations were high in channels upstream of in-channel wetlands (on average 13.9 mg L^{-1}). In contrast, nitrate concentrations were lower in channels downstream of in-channel wetlands (on average 12.6 mg L^{-1}) and were very low in wetlands (on average 0 mg L^{-1}). Larger wetlands tended to have a greater effect on lowering downstream nitrate concentrations than smaller wetlands (Figures 7b and 7c). As flow increased, simulated nitrate concentrations increased and the extent of a wetland's effect of reducing downstream nitrate concentrations diminished. At high flow (Figure 7c), there was less spatial variability in simulated nitrate concentrations, where channels had consistently high concentrations (on average 16.7 mg L^{-1} upstream of in-channel wetlands and 17.1 mg L^{-1} downstream of in-channel wetlands) and wetlands exhibited a range of lower concentrations than channels (on average 2.2 mg L^{-1}).

We summarized the network-wide nitrate concentrations at each simulated flow by computing a length-averaged nitrate concentration throughout the network (wetlands were given a "length" equal to $\sqrt{W_{A,i}}$; Figure 7a). For this and all network-wide summary figures that follow, the black line corresponds to the calibrated conditions and the gray lines represent the sensitivity of the results to a $\pm$10% change in select parameters. For the Le Sueur Basin, the simulated network-averaged nitrate concentration increased with increasing flow. The simulated network-averaged nitrate concentration was largely insensitive to the $\pm$10% change in uncertain parameters (cluster of gray lines around the black line in Figure 7a) except for N^{rc}_{nom} (corresponding to the gray lines spread out from the others in Figure 7a). Changing N^{rc}_{nom} by $\pm$10% corresponded to roughly a $\pm$2% change in network-averaged nitrate concentration. The simulated nitrate mass flux at the basin outlet (computed as the product of nitrate concentration and flow discharge from the link at the basin outlet) also increased as flow increased, but by several orders of magnitude (Figure 7d).

Of the simulated nitrate delivered to a link, we assessed the fraction removed along the pathway from that link to the basin outlet (Figures 7f and 7g) to visualize the locations from which nitrate was removed from the system or, conversely, the locations delivering nitrate to the basin outlet. At low flow (Figure 7f), simulated nitrate contributions to the basin outlet were mostly confined to the largest and farthest downstream channels; roughly 80% of simulated nitrate inputs were removed and 20% were exported from the basin

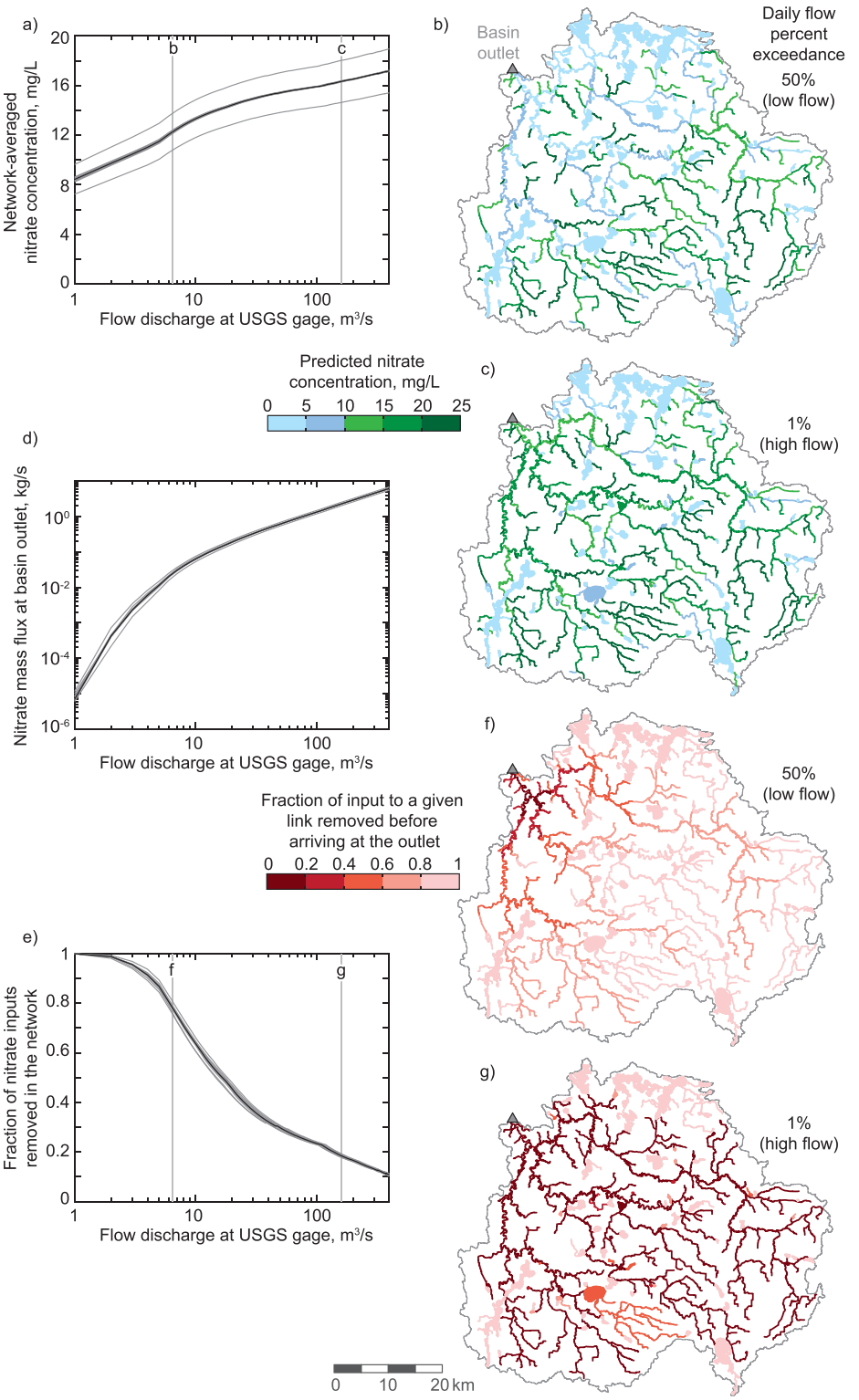

Figure 7. Simulated network-wide nitrate concentrations, loads, and removal. (a) Length-averaged nitrate concentration throughout the network; wetlands were given a "length" equal to $\sqrt{W_{A,i}}$. The black line corresponds to the calibrated conditions and the gray lines correspond to the results of the sensitivity analysis. Network-wide nitrate concentration at the (b) 50% (low flow) and (c) 1% (high flow) daily flow exceedance. (d) Nitrate mass flux at the basin outlet. (e) Fraction of nitrate inputs removed in the network. Fraction of input to a given link removed before arriving at the basin outlet at the (f) 50% and (g) 1% daily flow exceedance.

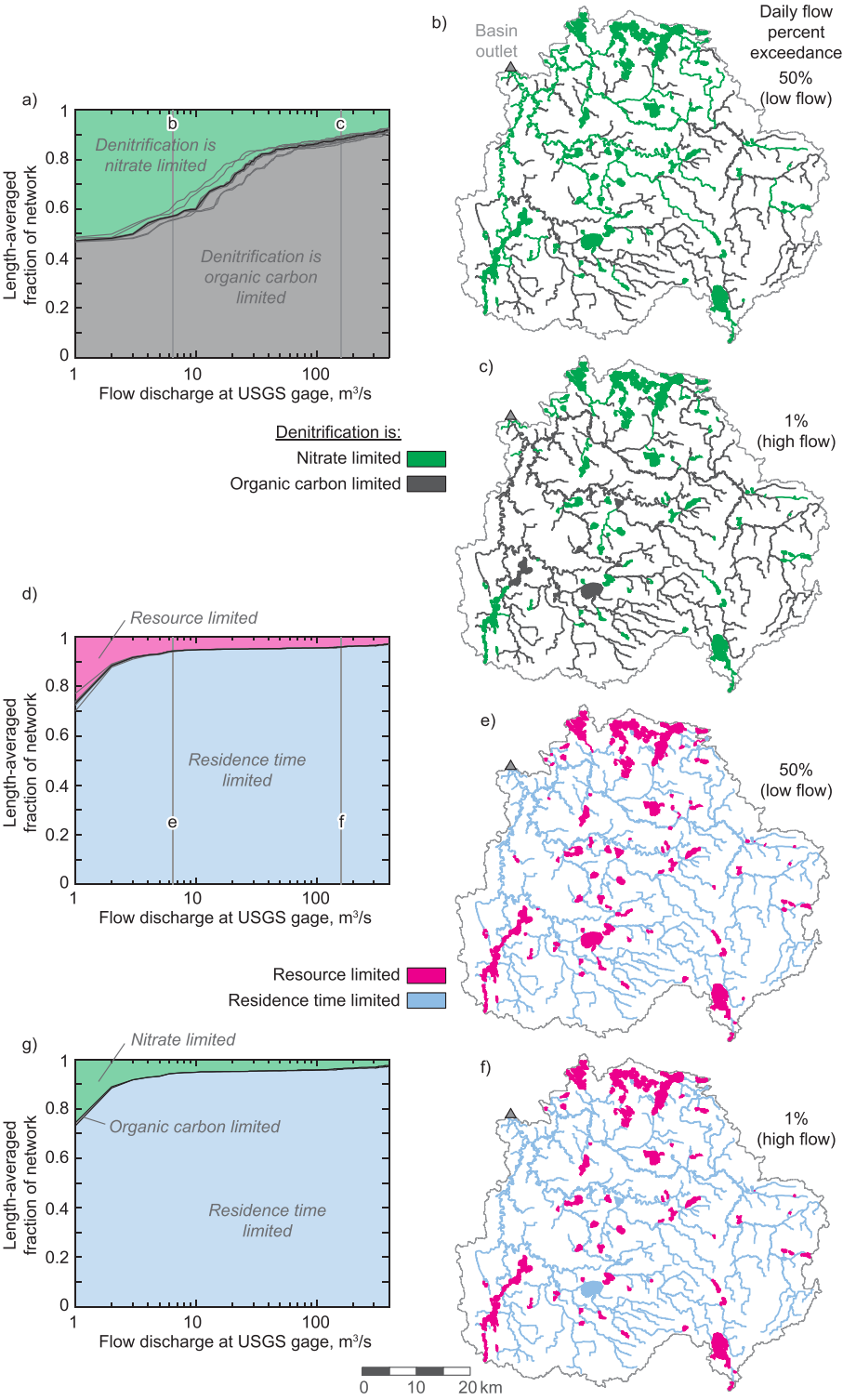

Figure 8. Simulated network-wide limitation on nitrate removal. (a) Length-averaged fraction of the network where denitrification is nitrate or organic carbon limited; wetlands were given a "length" equal to $\sqrt{W_{A,i}}$. The black line corresponds to the calibrated conditions and the gray lines correspond to the results of the sensitivity analysis. Network-wide resource limitation on nitrate removal at the (b) 50% (low flow) and (c) 1% (high flow) daily flow exceedance. (d) Length-averaged fraction of the network that is resource or residence time limited based on the Damköhler number Da_i. Network-wide resource or residence time limitation on nitrate removal at the (e) 50% and (f) 1% daily flow exceedance. (g) Length-average fraction of the network that is overall limited by nitrate, organic carbon, or residence time.

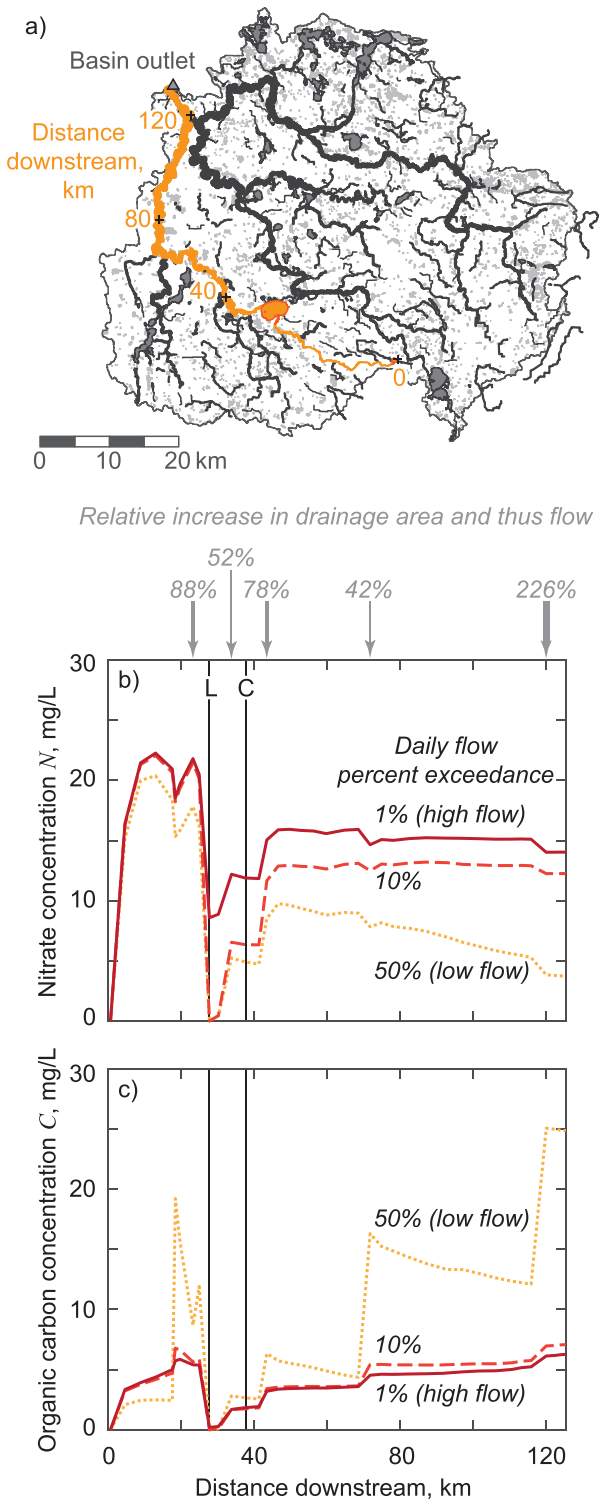

Figure 9. Simulated nitrate and organic carbon concentration along a pathway through the network. (a) Basin map showing highlighted pathway. (b) Nitrate concentration N_i and (b) organic carbon concentration C_i along the pathway. Vertical lines labeled "L" and "C" refer to the lake and channel, respectively, highlighted in Figure 10.

(Figure 7e). Nitrate originating from other areas of the basin was either intercepted and removed in wetlands, or had a long enough travel time, i.e., originated far enough away from the outlet that it was largely removed through in-channel denitrification at this particular low flow. At high flow (Figure 7g), a large proportion of the basin contributed nitrate to the basin outlet; roughly 20% of simulated nitrate inputs were removed and 80% were exported from the basin (Figure 7e). In general, wetlands were effective at removing nitrate across a wide range in flow conditions and thus often noticeably reduced simulated nitrate concentrations within them and for some distance downstream. Note that areas upstream of more prominent wetlands also rarely contributed nitrate to the basin outlet because their nitrate contributions were intercepted and denitrified.

In general, model simulations indicated that the resource limiting denitrification in channels was often organic carbon and in wetlands was often nitrate (when only considering $C_i : N_i$, Figures 8b and 8c). At low flow (Figure 8b), there was a greater proportion of the network for which denitrification was nitrate limited; roughly half of the network (Figure 8a). Typically, simulated denitrification was nitrate limited in channels downstream of wetlands that produced a lot of organic carbon. In contrast, at high flow (Figure 8c), denitrification was organic carbon limited in many of the links (including some wetlands); roughly 90% of the network (Figure 8a).

The overall limitation on nitrate removal in wetlands was often resource supply (nitrate or organic carbon) and in channels was often residence time (when only considering Da_i, Figures 8d–8f). A few wetlands switched from a resource limitation at low flow (Figure 8e) to a residence time limitation at high flow (Figure 8f). For most simulated flows, residence time limited nitrate removal throughout roughly 90% of the network (by length; Figures 8d and 8g). When the overall limitation on nitrate removal was resource supply it tended to be nitrate limited (when considering both Da_i and $C_i : N_i$, Figure 8g and also comparing Figures 8e and 8f with Figures 8b and 8c). Only a very small fraction of the network had organic carbon as the overall limitation on nitrate removal (Figure 8g). These simulations show that for the Le Sueur Basin, residence time was the primary limitation on nitrate removal despite a paucity of organic carbon for denitrification.

5.3. Flow-Dependent Regime Shifts in the Limitation on Nitrate Removal

Within the Le Sueur Basin, simulated nitrate and organic carbon concentrations are shown along a profile through the network at the 50% (low flow), 10%, and 1% (high flow) daily flow percent exceedance (Figure 9). A relatively large shallow lake (surface area of 8.1 km^2, average depth of 0.9 m) sits roughly 30 km downstream along the profile (a lake for purposes of our discussion is a wetland with a low fraction of emergent vegetation $f_{em,i}$). This lake did not generate much organic carbon ($f_{em,i} = 0.24$; see Figure 2), but was effective at reducing simulated nitrate concentrations due to relatively long residence times; particularly at low flow when simulated nitrate concentrations out of the lake were near zero. At high flow, the simulated nitrate concentration out of the lake abruptly increased to 10 mg L^{-1} as the lake transitioned from resource supply limited to residence time limited (Figures 10b and 10c). A major wetland complex delivered a large amount of

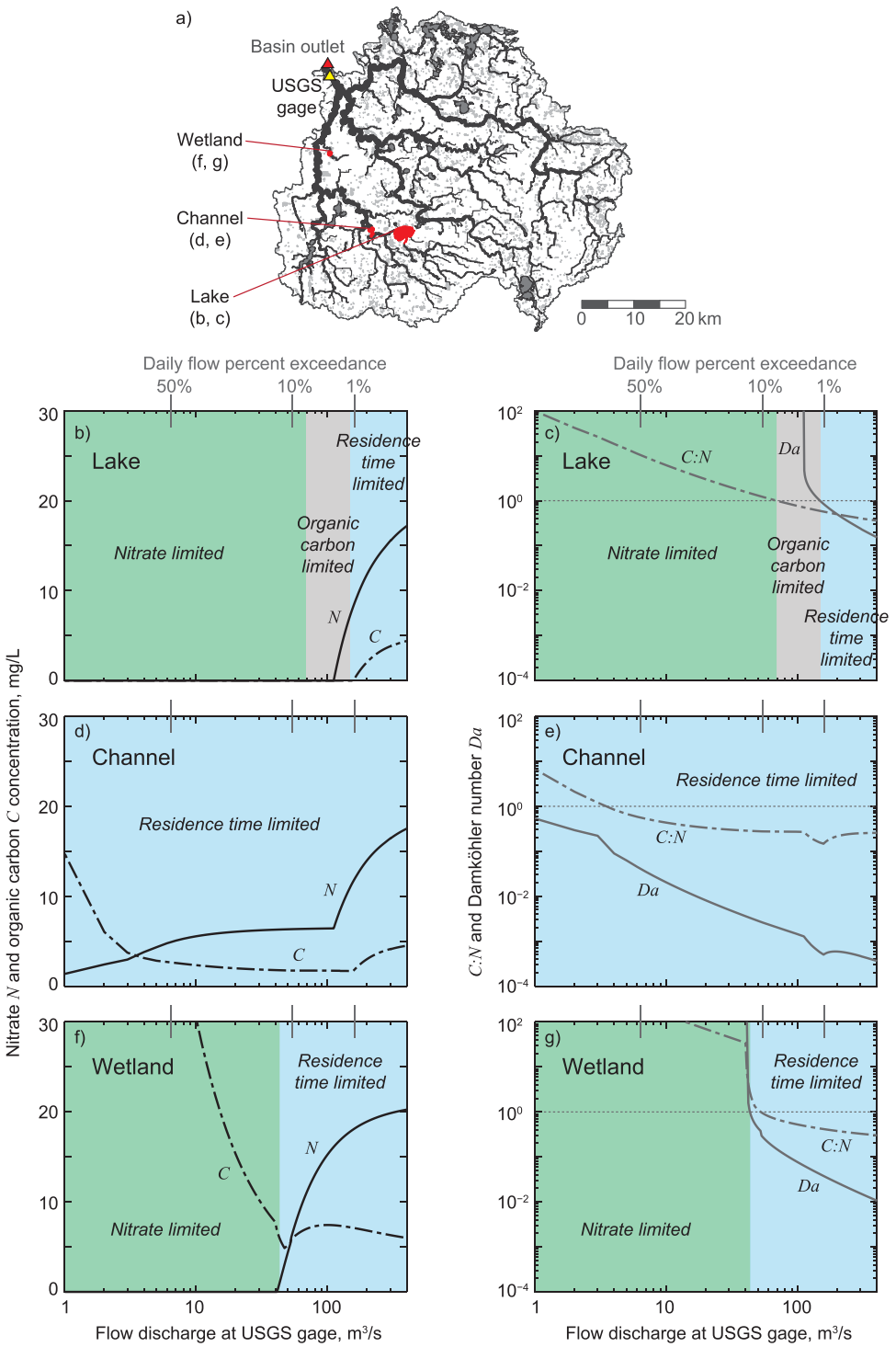

Figure 10. Simulated flow-dependent regime shifts in the limitation on nitrate removal; typically, with increasing flow the limitation shifts from nitrate concentration, to organic carbon availability, to residence time (flow; when transport out of a link is much faster than the denitrification reaction time scale). (a) Basin map showing highlighted links. (b, d, f) Nitrate concentration N_i and organic carbon concentration C_i, and (c, e, g) organic carbon to nitrate ratio $C_i : N_i$ and the Damköhler number Da_i (ratio of the transport time scale to the denitrification reaction time scale) versus flow for a (b, c) lake, (d, e) channel just downstream of the lake, and (f, g) wetland. Based on a simplified model, a threshold value of one for $C_i : N_i$ sets the nitrate versus organic carbon limitation and for Da_i sets the resource versus residence time limitation.

organic carbon at roughly 70 km downstream along the profile (Figure 9b). Only at low flow did we see a substantial increase in simulated organic carbon concentration, which increased denitrification rates, and thereby reduced simulated nitrate concentrations; at high flow this effect became insignificant.

Simulated conditions within a lake, channel, and wetland are shown to illustrate the general behavior of each waterbody with increasing flow (Figure 10). Note that for this example, the channel is located roughly 10 km downstream of the lake. For lakes, which in the model have less vegetation and generate much less organic carbon than wetlands, the limitation on nitrate removal shifted from nitrate supply, to organic

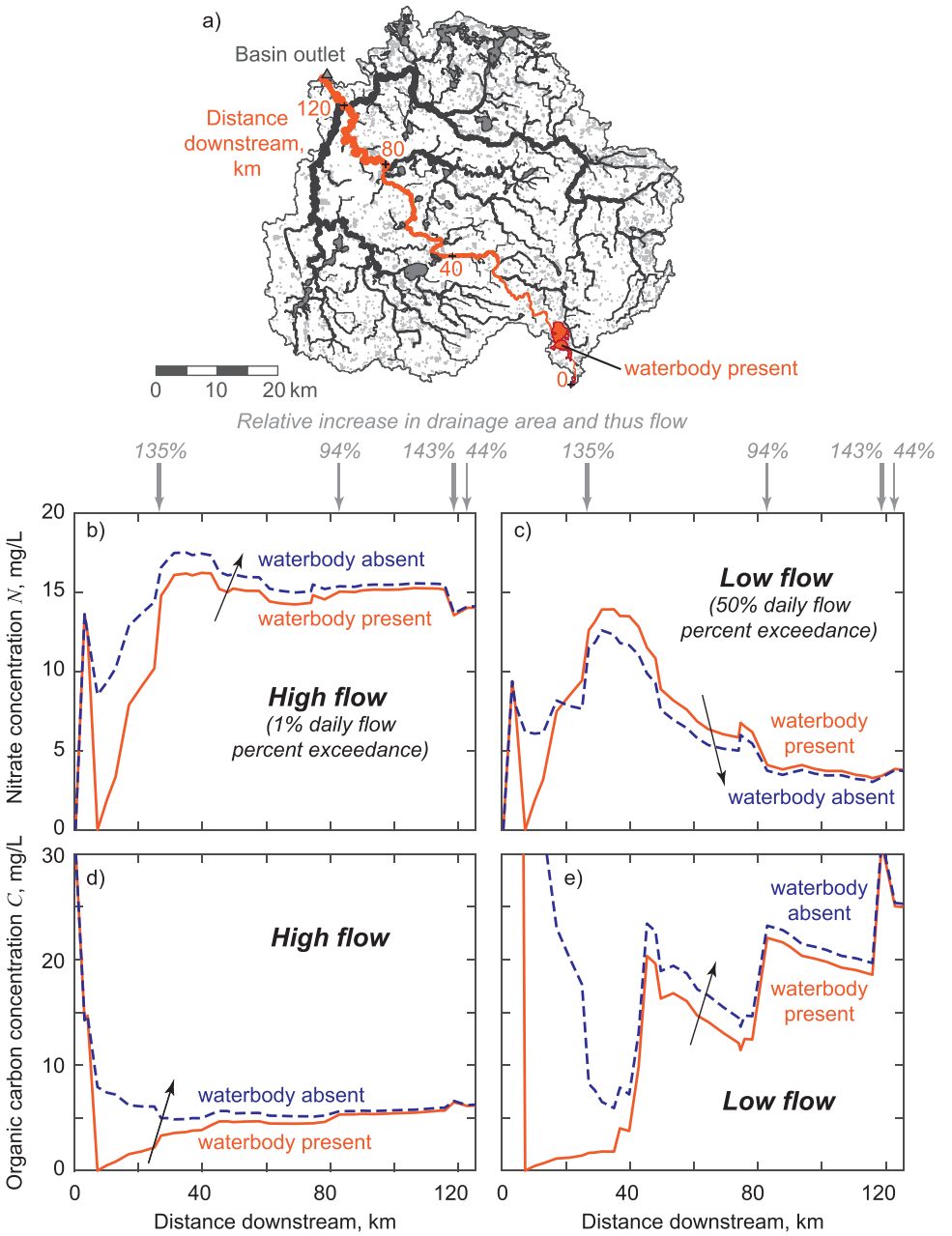

Figure 11. Conditions under which the presence or absence of a waterbody could give rise to unexpected behavior: when the absence of a lake downstream of a wetland can reduce downstream nitrate concentrations. (a) Highlighted pathway through the wetland-river network in the Le Sueur Basin along which further results are shown: (b, c) Nitrate concentration N_i and (d, e) organic carbon concentration C_i at the (b, d) 1% (high flow) and (c, e) 50% (low flow) daily flow percent exceedance. Conditions with the waterbody (lake) present (roughly 10 km downstream along the profile) are shown with a solid orange line whereas with the waterbody absent are shown with a dashed blue line.

carbon supply, to residence time as flow increased (Figures 10b and 10c). Simulated nitrate concentrations increased significantly as the flow approached the threshold in resource supply/residence time limitation (i.e., when the Damköhler number equaled one, Figure 10c). This is because nitrate was being transported through the waterbody faster than it could be removed by the denitrification process. In contrast, nitrate removal was most often residence time limited in channels (Figures 10d and 10e), and nitrate concentrations gradually increased across a range of simulated flows (such as for low to moderate flows shown in Figure 10d). However, an abrupt increase in simulated nitrate concentration in the channel (Figure 10d) occurred as a result of the downstream propagation, under the simulated steady state conditions, of the increase in simulated nitrate concentration in the upstream lake (Figure 10b). Thus, when a lake (or wetland) crosses a threshold in resource supply/residence time limitation, downstream waterbodies can become affected in otherwise seemingly unexpected ways. Unlike lakes, wetlands generated substantial organic carbon and the limitation on nitrate removal typically shifted directly from nitrate to residence time as flow increased (Figures 10f and 10g). When a wetland or lake became residence time limited, simulated nitrate concentrations in the waterbody, as well as in downstream channels, increased significantly (Figure 10). The shift in limitation on nitrate removal, in particular from resource supply to residence time limitation, resulted in a significant increase in simulated nitrate concentrations. The particular flow condition at which a waterbody undergoes a regime shift in the limitation on nitrate removal will vary depending on characteristics of the waterbody and its location in the network.

5.4. Location of Wetlands Matters

In hierarchically connected systems, there is a large potential for spatial interactions of connected waterbodies. The importance of spatial interactions has been discussed (Fergus et al., 2017; Jones, 2010) and investigated in the context of a chain of lakes (Kling et al., 2000; Soranno et al., 1999), but overall this concept has been largely understudied. We use another profile through the Le Sueur Basin to reveal the mechanisms by which the relative spatial position of multiple waterbodies affects network-wide nitrate removal (Figure 11). This profile starts at a wetland ($f_{em,i} = 0.54$; see Figure 2) and we consider the presence and absence of a large lake ($f_{em,i} = 0.12$; see Figure 2) located roughly 10 km downstream (Figure 11a). In the model, the upstream wetland generated and exported a considerable amount of organic carbon which was completely utilized within the downstream lake via denitrification to completely remove nitrate (solid orange lines, Figures 11b–11e). Simulated nitrate concentrations downstream of this lake progressively increased as nitrate was added from the surrounding landscape.

In the absence of the lake (dashed blue lines, Figures 11b–11e) and at its former location 10 km downstream along the profile, nitrate was no longer significantly removed (Figures 11b and 11c). At high flow, downstream nitrate concentrations were higher, as expected (Figure 11b). However, at low flow, downstream nitrate concentrations were unexpectedly lower (Figure 11c). This occurred because in the absence of the lake, higher organic carbon concentrations propagated downstream thereby increasing denitrification rates in these reaches and thus reducing downstream nitrate concentrations. This one modification was too far away to affect simulated nitrate concentrations at the basin outlet and thus simulated loads delivered from the basin. This example illustrates how efforts to reduce watershed-scale nitrate concentrations and loads by restoring wetlands need to carefully consider the cascade of biogeochemical changes that propagate through the network in response to the spatial positioning of a suite of restored wetlands.

6. Discussion

6.1. Limitations and Further Extensions

The present model is a first step toward understanding how a suite of wetlands interacts dynamically within a hierarchically connected river network to dictate the system biogeochemistry and thus nitrate removal at the watershed scale. By employing a simple representation of biogeochemical transformations, we developed a model that captures the behavior of nitrate in a large, spatially complex watershed yet was computationally manageable and flexible. Our model has several limitations however, and here we discuss only the major ones. First, for the model to be applied to a wider set of conditions, including warmer conditions within the same climate, it would be necessary to extend the representation of nitrogen dynamics to include, at a minimum, vegetative assimilation, nitrogen mineralization, and nitrification (Payne et al., 2014). In particular, nitrogen assimilation can be substantial in the summer, and in wetlands, assimilated nitrogen

is likely to be ultimately removed given favorable conditions for retention and denitrification. These processes are not captured in the model. This model also does not yet include information for generation and cycling of organic nitrogen and ammonium, which can represent loss pathways for nitrogen from wetlands (Vymazal, 2007).

A considerable source of uncertainty in our model might result from our representation of organic carbon inputs and the dependence of denitrification on organic carbon. Organic carbon is a required energy source for denitrification; DOC, used to represent organic carbon in the model, represents a wide range of materials with highly variable bioavailability (Mineau et al., 2016; Wilson & Xenopoulos, 2008). Furthermore, DOC is utilized in heterotrophic pathways besides denitrification as well as subject to photodegradation (or conversely photopriming), all of which can alter its availability for denitrification (Koehler et al., 2014; Lapierre et al., 2013; Vachon et al., 2017). Further research is needed toward the functional link between DOC and denitrification rates under DOC limited conditions.

Finally, lakes are included in this model as wetlands. In the Le Sueur Basin, the majority of lakes are shallow, and have an abundance of aquatic plants. These shallow lakes are functionally very similar to wetlands. However in deep lakes, biogeochemical processes occurring in the water column become important and can greatly influence elemental cycles. For example, autotrophic assimilation of nitrate and subsequent transfer of organic nitrogen to sediments may be important, yet indirect, regulators of ecosystem denitrification (Finlay et al., 2013).

6.2. Complexity and Spatial Context of Wetlands

Herein, we have developed a watershed-scale model focused on aquatic nitrate transport, dilution, and removal via denitrification. To properly account for denitrification in agricultural landscapes, where organic carbon typically limits denitrification (Bernhardt & Likens, 2002; Hansen et al., 2016; Inwood et al., 2007; Zarnetske et al., 2011), we also tracked aquatic organic carbon and the effect resource supply limitation had on denitrification rates. Overall, these dynamics represented a relatively simple conceptualization of denitrification (e.g., Figure 6). Complexity emerged largely from network structure. That is, activating these dynamics on a hierarchical wetland-river network with spatially heterogeneous attributes resulted in some "surprises" (see section 5.4) due to biogeochemical feedbacks and cascading dynamics within the system.

Considered in isolation, an individual wetland can alter downstream denitrification rates (Figure 6c) and may undergo a flow-dependent regime shift in the limitation on nitrate removal (Figure 10b-c and 10f-g). The strength and timing of these effects will depend on the characteristics of an individual wetland (e.g., size and amount of vegetation) and its location in the network (e.g., upstream drainage area, which largely controls the flow discharge and integration of upstream nitrate and organic carbon inputs; proximity and connectivity to row-crop agriculture and nonagricultural, vegetated lands, which determines the local terrestrial nitrate and organic carbon inputs). Once we add spatial context to a collection of wetlands on a hierarchical river network, then we start to see more complexity emerging as upstream regime shifts in the limitation on nitrate removal cascade downstream to increased nitrate concentrations (Figure 6).

Thus, our modeling efforts illustrate that changes in the landscape can initiate a cascade of changes that will propagate through the watershed. For instance, historical wetlands throughout many Midwestern U.S. agricultural landscapes have been drained and effectively removed (Dahl & Allord, 1996). The terrestrial landscape itself has transitioned from prairie to hay and small grains then to corn and soybeans today, along with an increase in drainage via surface ditches and underground tiles (e.g., Foufoula-Georgiou et al., 2015). These changes in the landscape have helped establish high nitrate concentrations and loads in downstream waterbodies that are now the target of restoration efforts (e.g., MPCA, 2013). Current efforts toward this end have not been as effective as hoped (e.g., Minnesota Pollution Control Agency, 2014) because the spatial context and cascading effects of restoration efforts, which can now be revealed with our developed model, have not been adequately assessed.

In our analysis, we have summarized nitrate concentrations and loads into a set of curves that are characteristic of a particular landscape configuration (Figures 7a and 7d). Changes in the landscape will produce a different set of these characteristic curves. Some restoration strategies could be more effective at reducing nitrate loads exported from the basin than reducing basin-wide nitrate concentrations and vice versa. Our developed model and these characteristic curves are useful for assessing the impact of landscape changes

on nitrate concentrations and loads and for comparing restoration strategies. Furthermore, it is important to note that any landscape change aimed at reducing nitrate concentrations and/or loads will invariably affect other aspects of the system (e.g., water and sediment) and these aspects should be considered to obtain a holistic perspective.

6.3. Implications for Wetland Restoration

Our model has three key findings of importance to the design of wetland restorations.

1. Increasing residence time will have a larger influence on nitrate removal than increasing organic carbon. Although the supply of organic carbon often limits denitrification rates in agricultural basins (Bernhardt & Likens, 2002; Hansen et al., 2016; Inwood et al., 2007; Zarnetske et al., 2011), almost all locations (mostly channels) where denitrification rates were limited by the supply of organic carbon were also locations where nitrate removal via denitrification was more limited by residence time. As a first priority, resource managers should consider increasing residence times potentially by promoting the development of permeable bedforms along the streambed (Gomez-Velez et al., 2015), restoring lateral floodplain connectivity (Kiel & Cardenas, 2014), creating channel backwaters, or reducing the flow arriving from upstream (note these changes would also affect other ecosystem services, including sediment transport and deposition, which would need to be evaluated as part of the overall strategy). In conjunction, organic carbon should be increased for maximum nitrate removal efficiency.
2. Wetlands can essentially remove virtually all nitrate contributions from upstream areas of the basin if they are sized and spaced appropriately. Isolated wetlands typically intercept much smaller contributing areas and thus have a smaller effect on basin-wide nitrate concentrations than flow-through wetlands. Flow-through wetlands have a large capacity to remove nitrate across a wide range of hydraulic and nitrate loading conditions (Kadlec, 2012; Thiere et al., 2011).
3. Wetlands affect downstream nitrate concentrations by changing water chemistry, hydrology, and biogeochemical processing rates. The downstream extent of this "wetland effect" is dependent on flow, wetland characteristics, interactions of resource limitation, and network configuration.

7. Concluding Remarks and Future Work

Our watershed-scale, network-based model of nitrate-nitrogen and dissolved organic carbon concentration through a collection of wetlands within a river network showed that (1) the limitation on nitrate removal shifts between nitrate, organic carbon, and residence time and (2) the spatial context of wetland restorations is important because nonlinearities in the system can lead to unexpected changes in downstream biogeochemistry. The consequence is that in order to be effective, efforts to reduce watershed-scale nitrate concentrations and loads by restoring wetlands need to carefully consider the cascade of biogeochemical changes that are likely to propagate through the network. Specifically, in the Le Sueur Basin efforts should target increasing water residence time (by slowing the flow) instead of increasing organic carbon concentrations (which biogeochemically limit denitrification) to most effectively reduce nitrate concentrations and loads. Future work will use this network-based framework for assessing where and with what specifications to restore wetlands for reducing nitrate concentrations in and loads from the Le Sueur Basin. Furthermore, our model simulations have revealed a complex behavior of a wetland-river network system. Given the assumptions and limitations of our model, this simulated behavior presents new hypotheses to test with further field investigation.

Appendix A: Damköhler Number

The Damköhler number Da_i is a dimensionless number that relates the convective mass transport time scale to the biogeochemical reaction time scale (Pinay et al., 2015) as

$$Da_i = \frac{\tau_{trans,i}}{\tau_{react,i}} \tag{A1}$$

where $\tau_{trans,i}$ [T] is the convective mass transport time scale and $\tau_{react,i}$ [T] is the biogeochemical reaction time scale.

In the present formulation, the transport time scale is given by the travel time through a link t_i [T] as

$$\tau_{trans,i} = t_i \tag{A2}$$

The reaction time scale is often given as the inverse of the rate constant of a first-order decay equation k_i [T^{-1}] (Pinay et al., 2015) as

$$\tau_{react,i} = \frac{1}{k_i} \tag{A3}$$

However, the denitrification process in this formulation is much more complicated than simple first-order decay. Instead, we can use the model results to back-out an estimate of a rate constant approximating a first-order decay process as a characteristic denitrification reaction time scale.

We first write the solution to a first-order decay reaction as

$$N_{out,i} = N_{in,i} e^{-k_i t_i} \tag{A4}$$

where in the present formulation $N_{out,i}$ is the nitrate concentration out of a link, $N_{in,i}$ is the nitrate concentration into a link, k_i is the rate constant of the first-order decay equation, and t_i is the travel time through a link. We can rearrange equation (A4) to solve in terms of k_i as

$$k_i = -\frac{\ln\left(\frac{N_{out,i}}{N_{in,i}}\right)}{t_i} \tag{A5}$$

Thus, upon substituting equation (A5) into (A3) the reaction time scale becomes

$$\tau_{react,i} = -\frac{t_i}{\ln\left(\frac{N_{out,i}}{N_{in,i}}\right)} \tag{A6}$$

Finally, upon substituting equations (A2) and (A6) into equation (A1), the Damköhler number reduces to

$$Da_i = -\ln\left(\frac{N_{out,i}}{N_{in,i}}\right) \tag{A7}$$

which is straightforward to calculate from the model results.

Notation

ACC	accuracy computed from a confusion matrix.
A_{gage}	upstream drainage area at the USGS Rapidan gage [L^2; where L is a unit of length].
A_i	upstream drainage area of link i [L^2].
a_i	directly contributing area to link i [L^2].
$\mathcal{A}_{c,i}$	wetted area in channel link i where denitrification takes place [L^2].
$\mathcal{A}_{vw,i}$	areal extent of emergent vegetation in wetland link i [L^2].
$\mathcal{A}_{w,i}$	wetted area in wetland link i where denitrification takes place [L^2].
B_{gage}	average width of channel at the USGS Rapidan gage [L].
B_i	average width of channel link i [L].
$C_{a,i}$	dissolved organic carbon concentration contributed from the directly contributing area a_i of link i [$M\,L^{-3}$; where M is a unit of mass].
C_i	dissolved organic carbon concentration in link i [$M\,L^{-3}$].
$C_{in,i}$	dissolved organic carbon concentration into link i [$M\,L^{-3}$].
C^m_{nom}	nominal dissolved organic carbon concentration input from land-use m [$M\,L^{-3}$].
C^{rc}_{nom}	nominal dissolved organic carbon concentration input from row-crop agriculture [$M\,L^{-3}$].
C^{v}_{nom}	nominal dissolved organic carbon concentration input from nonagricultural, vegetated land [$M\,L^{-3}$].
$C_{out,i}$	dissolved organic carbon concentration out of link i [$M\,L^{-3}$].
$C_{out,j}$	dissolved organic carbon concentration out of upstream link j [$M\,L^{-3}$].
$C_{out,k}$	dissolved organic carbon concentration out of upstream link k [$M\,L^{-3}$].
Da_i	Damköhler number of link i.

FN number of false negatives.
FP number of false positives.
$f^m_{a,i}$ fraction of the directly contributing area a_i classified as land-use m that drains to link i without being intercepted by isolated wetlands.
$f^{rc}_{a,i}$ fraction of the directly contributing area a_i classified as row-crop agriculture rc that drains to link i without being intercepted by isolated wetlands.
$f^v_{a,i}$ fraction of the directly contributing area a_i classified as nonagricultural, vegetated land v that drains to link i without being intercepted by isolated wetlands.
$f_{em,i}$ fraction of emergent vegetation in wetland link i.
i index of a link of the network.
$J_{den,i}$ denitrification flux in link i [$M\,L^{-2}\,T^{-1}$; where T is a unit of time].
J_{prod} vegetation organic carbon production flux [$M\,L^{-2}\,T^{-1}$].
j index of a link directly upstream of link i.
k index of a link directly upstream of link i.
k_i rate constant of a first-order decay equation [T^{-1}].
ℓ_i length of channel link i [L].
MCC Matthews correlation coefficient computed from a confusion matrix.
m index of land use class.
$N_{a,i}$ nitrate concentration contributed from the directly contributing area a_i of link i [$M\,L^{-3}$].
N_i nitrate concentration in link i [$M\,L^{-3}$].
$N_{in,i}$ nitrate concentration into link i [$M\,L^{-3}$].
N^m_{nom} nominal nitrate concentration input from land-use m [$M\,L^{-3}$].
N^{rc}_{nom} nominal nitrate concentration input from row-crop agriculture [$M\,L^{-3}$].
$N_{out,i}$ nitrate concentration out of link i [$M\,L^{-3}$].
$N_{out,j}$ nitrate concentration out of upstream link j [$M\,L^{-3}$].
$N_{out,k}$ nitrate concentration out of upstream link k [$M\,L^{-3}$].
$Q_{a,i}$ flow discharge contributed from the directly contributing area a_i of link i [$L^3\,T^{-1}$].
Q_{gage} flow discharge at the USGS Rapidan gage [$L^3\,T^{-1}$].
Q_i flow discharge through link i [$L^3\,T^{-1}$].
Q_j flow discharge through upstream link j [$L^3\,T^{-1}$].
Q_k flow discharge through upstream link k [$L^3\,T^{-1}$].
rc index denoting the row-crop agricultural land use class.
TN number of true negatives.
TP number of true positives.
t_i travel time through link i [T].
v index denoting the nonagricultural, vegetated land use class.
$W_{A,i}$ surface area of wetland link i [L^2].
λ parameter of the dissolved organic carbon-limited denitrification flux equation.
$\tau_{react,i}$ biogeochemical reaction (denitrification) time scale of link i [T].
$\tau_{trans,i}$ convective mass transport time scale (residence time) of link i [T].

Acknowledgments
This research was funded by NSF grant EAR-1209402 under the Water Sustainability and Climate Program (WSC): REACH (REsilience under Accelerated CHange) and benefited from collaborations made possible by NSF grant EAR-1242458 under Science Across Virtual Institutes (SAVI): LIFE (Linked Institutions for Future Earth). J.A.C. acknowledges support provided by an Interdisciplinary Doctoral Fellowship through the University of Minnesota Graduate School and Institute on the Environment and also an Edward Silberman Fellowship through the St. Anthony Falls Laboratory. A.T.H. acknowledges support provided by NSF grant EAR-1415206 under the Science, Engineering and Education for Sustainability (SEES) Fellow Program. Nitrate and DOC data are available through Dolph et al. (2017a). All model codes have been made freely available in the Community Surface Dynamics Modeling System (CSDMS) under the model heading "Nitrate Network Model" (http://csdms.colorado.edu/wiki/Model:Nitrate_Network_Model). The model has also been packaged as an interactive, online computer-simulation tool for educational purposes for users to explore the impact of land-management practices on nitrate concentrations and loads in a subbasin of the Le Sueur Basin (http://maps.umn.edu/le-sueur-nitrates/).

References

Alexander, R. B., Böhlke, J. K., Boyer, E. W., David, M. B., Harvey, J. W., Mulholland, P. J., et al. (2009). Dynamic modeling of nitrogen losses in river networks unravels the coupled effects of hydrological and biogeochemical processes. *Biogeochemistry*, *93*(1–2), 91–116. https://doi.org/10.1007/s10533-008-9274-8

Alexander, R. B., Smith, R. A., & Schwarz, G. E. (2000). Effect of stream channel size on the delivery of nitrogen to the Gulf of Mexico. *Nature*, *403*, 758–761. https://doi.org/10.1038/35001562

Arango, C. P., Tank, J. L., Schaller, J. L., Royer, T. V., Bernot, M. J., & David, M. B. (2007). Benthic organic carbon influences denitrification in streams with high nitrate concentration. *Freshwater Biology*, *52*(7), 1210–1222. https://doi.org/10.1111/j.1365-2427.2007.01758.x

Ayalew, T. B., Krajewski, W. F., & Mantilla, R. (2015). Analyzing the effects of excess rainfall properties on the scaling structure of peak discharges: Insights from a mesoscale river basin. *Water Resources Research*, *51*, 3900–3921. https://doi.org/10.1002/2014WR016258

Baron, J. S., Hall, E. K., Nolan, B. T., Finlay, J. C., Bernhardt, E. S., Harrison, J. A., et al. (2013). The interactive effects of excess reactive nitrogen and climate change on aquatic ecosystems and water resources of the United States. *Biogeochemistry*, *114*(1), 71–92. https://doi.org/10.1007/s10533-012-9788-y

Battye, W., Aneja, V. P., & Schlesinger, W. H. (2017). Is nitrogen the next carbon? *Earth's Future*, *5*, 894–904. https://doi.org/10.1002/2017EF000592

Bernhardt, E. S., & Likens, G. E. (2002). Dissolved organic carbon enrichment alters nitrogen dynamics in a forest stream. *Ecology*, *83*(6), 1689–1700. https://doi.org/10.1890/0012-9658(2002)083[1689:DOCEAN]2.0.CO;2

Bernot, M. J., Tank, J. L., Royer, T. V., & David, M. B. (2006). Nutrient uptake in streams draining agricultural catchments of the midwestern United States. *Freshwater Biology*, *51*(3), 499–509. https://doi.org/10.1111/j.1365-2427.2006.01508.x

Bertilsson, S., & Jones, J. B., Jr. (2003). Supply of dissolved organic matter in aquatic ecosystems: Autochthonous sources. In S. E. G. Findlay & R. L. Sinsabaugh (Eds.), *Aquatic ecosystems: Interactivity of dissolved organic matter* (pp. 3–19). San Diego, CA: Academic Press.

Birgand, F., Skaggs, R. W., Chescheir, G. M., & Gilliam, J. W. (2007). Nitrogen removal in streams of agricultural catchments—A literature review. *Critical Reviews in Environmental Science and Technology*, *37*(5), 381–487. https://doi.org/10.1080/10643380600966426

Bohlke, J. K., Antweiler, R. C., Harvey, J. W., Laursen, A. E., Smith, L. K., Smith, R. L., et al. (2009). Multi-scale measurements and modeling of denitrification in streams with varying flow and nitrate concentration in the upper Mississippi River Basin, USA. *Biogeochemistry*, *93*(1–2), 117–141. https://doi.org/10.1007/s10533-008-9282-8

Botter, G., Settin, T., Marani, M., & Rinaldo, A. (2006). A stochastic model of nitrate transport and cycling at basin scale. *Water Resources Research*, *42*, W04415. https://doi.org/10.1029/2005WR004599

Butman, D., Stackpoole, S., Stets, E., McDonald, C. P., Clow, D. W., & Striegl, R. G. (2016). Aquatic carbon cycling in the conterminous United States and implications for terrestrial carbon accounting. *Proceedings of the National Academy of Sciences of the United States of America*, *113*(1), 58–63. https://doi.org/10.1073/pnas.1512651112

Cohen, M. J., Creed, I. F., Alexander, L., Basu, N. B., Calhoun, A. J. K., Craft, C., et al. (2016). Do geographically isolated wetlands influence landscape functions? *Proceedings of the National Academy of Sciences of the United States of America*, *113*(8), 1978–1986. https://doi.org/10.1073/pnas.1512650113

Cowardin, L. M., Carter, V., Golet, F. C., & LaRoe, E. T. (1979). Classification of wetland and deepwater habitats of the United States (Rep. FWS/OBS-79/31, 131 pp.). Washington, DC: U.S. Fish and Wildlife Service.

Crumpton, W. G. (2001). Using wetlands for water quality improvement in agricultural watersheds; the importance of a watershed scale approach. *Water Science and Technology*, *44*(11–12), 559–564.

Crumpton, W. G., Stenback, G. A., Miller, B. A., & Helmers, M. J. (2006). *Potential benefits of wetland filters for tile drainage systems: Impact on nitrate loads to Mississippi River subbasins* (Ecology, Evolution and Organismal Biology Rep. 2, 36 pp.). Ames: Iowa State University.

Czuba, J. A., & Foufoula-Georgiou, E. (2014). A network-based framework for identifying potential synchronizations and amplifications of sediment delivery in river basins. *Water Resources Research*, *50*, 3826–3851. https://doi.org/10.1002/2013WR014227

Czuba, J. A., & Foufoula-Georgiou, E. (2015). Dynamic connectivity in a fluvial network for identifying hotspots of geomorphic change. *Water Resources Research*, *51*, 1401–1421. https://doi.org/10.1002/2014WR016139

Dahl, T. E., & Allord, G. J. (1996). History of wetlands in the conterminous United States. In *National water summary on wetland resources* (Water Supply Pap. 2425). Reston, VA: U.S. Geological Survey. Retrieved from http://water.usgs.gov/nwsum/WSP2425/history.html

Dalzell, B. J., King, J. Y., Mulla, D. J., Finlay, J. C., & Sands, G. R. (2011). Influence of subsurface drainage on quantity and quality of dissolved organic matter export from agricultural landscapes. *Journal of Geophysical Research*, *116*, G02023. https://doi.org/10.1029/2010JG001540

Davis, C. A., Ward, A. S., Burgin, A. J., Loecke, T. D., Riveros-Iregui, D. A., Schnoebelen, D. J., et al. (2014). Antecedent moisture controls on stream nitrate flux in an agricultural watershed. *Journal of Environmental Quality*, *43*(4), 1494. https://doi.org/10.2134/jeq2013.11.0438

Dolph, C. L., Hansen, A. T., & Finlay, J. C. (2017b). Flow-related dynamics in suspended algal biomass and its contribution to suspended particulate matter in an agricultural river network of the Minnesota River Basin, USA. *Hydrobiologia*, *785*(1), 127–147. https://doi.org/10.1007/s10750-016-2911-7

Dolph, C. L., Hansen, A. T., Kemmitt, K. L., Janke, B., Rorer, M., Winikoff, S., et al. (2017a). *Characterization of streams and rivers in the Minnesota River Basin Critical Observatory: Water chemistry and biological field collections, 2013–2016*. Data Repository for the University of Minnesota. Retrieved from https://doi.org/10.13020/D6FH44

Donner, S. D., Coe, M. T., Lenters, J. D., Twine, T. E., & Foley, J. A. (2002). Modeling the impact of hydrological changes on nitrate transport in the Mississippi River Basin from 1955 to 1994. *Global Biogeochemical Cycles*, *16*(3). https://doi.org/10.1029/2001GB001396

Donner, S. D., & Scavia, D. (2007). How climate controls the flux of nitrogen by the Mississippi River and the development of hypoxia in the Gulf of Mexico. *Limnology and Oceanography*, *52*(2), 856–861. https://doi.org/10.4319/lo.2007.52.2.0856

Dubrovsky, N. M., Burow, K. R., Clark, G. M., Gronberg, J. M., Hamilton, P. A., Hitt, K. J., et al. (2010). The quality of our nations water—Nutrients in the nation's streams and groundwater, 1992–2004 (U.S. Geol. Surv. Circ. 1350, 174 pp.). Reston, VA: U.S. Geological Survey.

Duff, J. H., Tesoriero, A. J., Richardson, W. B., Strauss, E. A., & Munn, M. D. (2008). Whole-stream response to nitrate loading in three streams draining agricultural landscapes. *Journal of Environmental Quality*, *37*(3), 1133–1144. https://doi.org/10.2134/jeq2007.0187

Fawcett, T. (2006). An introduction to ROC analysis. *Pattern Recognition Letters*, *27*(8), 861–874. https://doi.org/10.1016/j.patrec.2005.10.010

Fergus, C. E., Lapierre, J. F., Oliver, S. K., Skaff, N. K., Cheruvelil, K. S., Webster, K., et al. (2017). The freshwater landscape: Lake, wetland, and stream abundance and connectivity at macroscales. *Ecosphere*, *8*(8), e01911. https://doi.org/10.1002/ecs2.1911

Findlay, S. E. G., & Sinsabaugh, R. L. (2003). *Aquatic ecosystems: Interactivity of dissolved organic matter* (512 pp.). San Diego, CA: Academic Press.

Finlay, J. C., Small, G. E., & Sterner, R. W. (2013). Human influences on nitrogen removal in lakes. *Science*, *342*(6155), 247–250. https://doi.org/10.1126/science.1242575

Fork, M. L., & Heffernan, J. B. (2014). Direct and indirect effects of dissolved organic matter source and concentration on denitrification in northern Florida rivers. *Ecosystems*, *17*(1), 14–28. https://doi.org/10.1007/s10021-013-9705-9

Foufoula-Georgiou, E., Takbiri, Z., Czuba, J. A., & Schwenk, J. (2015). The change of nature and the nature of change in agricultural landscapes: Hydrologic regime shifts modulate ecological transitions. *Water Resources Research*, *51*, 6649–6671. https://doi.org/10.1002/2015WR017637

Galloway, J. N., Townsend, A. R., Erisman, J. W., Bekunda, M., Cai, Z., Freney, J. R., et al. (2008). Transformation of the nitrogen cycle: Recent trends, questions, and potential solutions. *Science*, *320*(5878), 889–892. https://doi.org/10.1126/science.1136674

Gergel, S. E., Turner, M. G., Kratz, T. K., Applications, S. E., & Nov, N. (1999). Dissolved organic carbon as an indicator of the scale of watershed influence on lakes and rivers. *Ecological Applications*, *9*(4), 1377–1390. https://doi.org/10.1890/1051-0761(1999)009[1377:DOCAAI]2.0.CO;2

Golden, H. E., Creed, I. F., Ali, G., Basu, N. B., Neff, B. P., Rains, M. C., et al. (2017). Integrating geographically isolated wetlands into land management decisions. *Frontiers in Ecology and the Environment*, *15*(6), 319–327. https://doi.org/10.1002/fee.1504

Gomez-Velez, J. D., Harvey, J. W., Cardenas, M. B., & Kiel, B. (2015). Denitrification in the Mississippi River network controlled by flow through river bedforms. *Nature Geoscience*, *8*, 941–945. https://doi.org/10.1038/ngeo2567

Goolsby, D. A., Battaglin, W. A., Aulenbach, B. T., & Hooper, R. P. (2000). Nitrogen flux and sources in the Mississippi River Basin. *Science of the Total Environment*, *248*(2–3), 75–86. https://doi.org/10.1016/S0048-9697(99)00532-X

Gorham, E., Underwood, J., Janssens, J., Freedman, B., Maass, W., Waller, D., et al. (1998). The chemistry of streams in southwestern and central Nova Scotia, with particular reference to catchment vegetation and the influence of dissolved organic carbon primarily from wetlands. *Wetlands*, *18*(1), 115–132. https://doi.org/10.1007/BF03161449

Grebliunas, B. D., & Perry, W. L. (2016). Carbon limitation of sediment bacterial production and denitrification in high nitrate low carbon systems. *Environmental Earth Sciences*, *75*, 662. https://doi.org/10.1007/s12665-016-5464-1

Hansen, A. T., Dolph, C. L., Foufoula-Georgiou, E., & Finlay, J. C. (2018). Contribution of wetlands to nitrate removal at the watershed scale. *Nature Geoscience*, *11*, 127–132. https://doi.org/10.1038/s41561-017-0056-6

Hansen, A. T., Dolph, C. L., & Finlay, J. C. (2016). Do wetlands enhance downstream denitrification in agricultural landscapes? *Ecosphere*, *7*(10), e01516. https://doi.org/10.1002/ecs2.1516

Helton, A. M., Hall, R. O., Jr., & Bertuzzo, E. (2017). How network structure can affect nitrogen removal by streams. *Freshwater Biology*, *63*, 128–140. https://doi.org/10.1111/fwb.12990

Helton, A. M., Poole, G. C., Meyer, J. L., Wollheim, W. M., Peterson, B. J., Mulholland, P. J., et al. (2011). Thinking outside the channel: Modeling nitrogen cycling in networked river ecosystems. *Frontiers in Ecology and the Environment*, *9*(4), 229–238. https://doi.org/10.1890/080211

Homer, C. G., Dewitz, J. A., Yang, L., Jin, S., Danielson, P., Xian, G., et al. (2015). Completion of the 2011 National Land Cover Database for the conterminous United States—Representing a decade of land cover change information. *Photogrammetric Engineering and Remote Sensing*, *81*(5), 345–354. https://doi.org/10.1016/S0099-1112(15)30100-2

Horizon Systems. (2014). *NHDPlus version 2*. Herndon, VA: Horizon Systems Corporation. Retrieved from http://www.horizon-systems.com/NHDPlus/NHDPlusV2_home.php

Howarth, R., Swaney, D., Billen, G., Garnier, J., Hong, B., Humborg, C., et al. (2012). Nitrogen fluxes from the landscape are controlled by net anthropogenic nitrogen inputs and by climate. *Frontiers in Ecology and the Environment*, *10*(1), 37–43. https://doi.org/10.1890/100178

Hubbard, L., Kolpin, D. W., Kalkhoff, S. J., & Robertson, D. M. (2011). Nutrient and sediment concentrations and corresponding loads during the historic June 2008 flooding in eastern Iowa. *Journal of Environmental Quality*, *40*, 166–175. https://doi.org/10.2134/jeq2010.0257

Inwood, S. E., Tank, J. L., & Bernot, M. J. (2007). Factors controlling sediment denitrification in midwestern streams of varying land use. *Microbial Ecology*, *53*(2), 247–258. https://doi.org/10.1007/s00248-006-9104-2

Johnston, C. A. (1991). Sediment and nutrient retention by freshwater wetlands: Effects on surface water quality. *Critical Reviews in Environmental Control*, *21*(5–6), 491–565. https://doi.org/10.1080/10643389109388425

Jones, N. E. (2010). Incorporating lakes within the river discontinuum: Longitudinal changes in ecological characteristics in stream-lake networks. *Canadian Journal of Fisheries and Aquatic Sciences*, *67*(8), 1350–1362. https://doi.org/10.1139/F10-069

Jordan, S. J., Stoffer, J., & Nestlerode, J. A. (2011). Wetlands as sinks for reactive nitrogen at continental and global scales: A meta-analysis. *Ecosystems*, *14*(1), 144–155. https://doi.org/10.1007/s10021-010-9400-z

Juckers, M., Williams, C. J., & Xenopoulos, M. A. (2013). Land-use effects on resource net flux rates and oxygen demand in stream sediments. *Freshwater Biology*, *58*(7), 1405–1415. https://doi.org/10.1111/fwb.12136

Kadlec, R. H. (2012). Constructed marshes for nitrate removal. *Critical Reviews in Environmental Science and Technology*, *42*(9), 934–1005. https://doi.org/10.1080/10643389.2010.534711

Kalkhoff, S. J., Hubbard, L. E., Tomer, M. D., & James, D. E. (2016). Effect of variable annual precipitation and nutrient input on nitrogen and phosphorus transport from two Midwestern agricultural watersheds. *Science of the Total Environment*, *559*(3), 53–62. https://doi.org/10.1016/j.scitotenv.2016.03.127

Keeler, B. L., Gourevitch, J. D., Polasky, S., Isbell, F., Tessum, C. W., Hill, J. D., et al. (2016). The social costs of nitrogen. *Science Advances*, *2*(10), e1600219. https://doi.org/10.1126/sciadv.1600219

Kiel, B. A., & Cardenas, M. B. (2014). Lateral hyporheic exchange throughout the Mississippi River network. *Nature Geoscience*, *7*, 413–417. https://doi.org/10.1038/ngeo2157

Kling, G. W., Kipphut, G. W., Miller, M. M., & O'Brien, W. J. (2000). Integration of lakes and streams in a landscape perspective: The importance of material processing on spatial patterns and temporal coherence. *Freshwater Biology*, *43*(3), 477–497. https://doi.org/10.1046/j.1365-2427.2000.00515.x

Knowles, R. (1982). Denitrification. *Microbiological Reviews*, *46*(1), 43–70.

Koehler, B., Landelius, T., Weyhenmeyer, G. A., Machida, N., & Tranvik, L. J. (2014). Sunlight-induced carbon dioxide emissions from inland waters. *Global Biogeochemical Cycles*, *28*, 696–711. https://doi.org/10.1002/2014GB004850

Kovacic, D. A., David, M. B., Gentry, L. E., Starks, K. M., & Cooke, R. A. (2000). Effectiveness of constructed wetlands in reducing nitrogen and phosphorus export from agricultural tile drainage. *Journal of Environmental Quality*, *29*(4), 1262–1274. https://doi.org/10.2134/jeq2000.00472425002900040033x

Kreiling, R. M., Richardson, W. B., Cavanaugh, J. C., & Bartsch, L. A. (2010). Summer nitrate uptake and denitrification in an upper Mississippi River backwater lake: The role of rooted aquatic vegetation. *Biogeochemistry*, *104*(1–3), 309–324. https://doi.org/10.1007/s10533-010-9503-9

Lapierre, J.-F., Guillemette, F., Berggren, M., & del Giorgio, P. A. (2013). Increases in terrestrially derived carbon stimulate organic carbon processing and CO_2 emissions in boreal aquatic ecosystems. *Nature Communications*, *4*, 2972. https://doi.org/10.1038/ncomms3972

Leopold, L. B., & Maddock, T., Jr. (1953). *The hydraulic geometry of stream channels and some physiographic implications* (Prof. Pap. 252, 57 pp.). Washington, DC: U. S. Geological Survey.

McKay, L., Bondelid, T., Dewald, T., Johnston, J., Moore, R., & Rea, A. (2012). *NHDPlus version 2: User guide*. Washington, DC: U.S. Environmental Protection Agency. Retrieved from ftp://ftp.horizon-systems.com/NHDPlus/NHDPlusV21/Documentation/NHDPlusV2_User_Guide.pdf

Mineau, M. M., Wollheim, W. M., Buffam, I., Findlay, S. E. G., Hall, R. O., Jr., Hotchkiss, E. R., et al. (2016). Dissolved organic carbon uptake in streams: A review and assessment of reach-scale measurements. *Journal of Geophysical Research: Biogeosciences*, *121*, 2019–2029. https://doi.org/10.1002/2015JG003204

Minnesota Department of Natural Resources. (2015). *National wetland inventory update for Minnesota*. Minnesota Geospatial Commons. Retrieved from https://gisdata.mn.gov/dataset/water-nat-wetlands-inv-2009-2014

Minnesota Pollution Control Agency. (2014). *The Minnesota nutrient reduction strategy* (doc. wq-s1–80, 348 pp.). St. Paul, MN:, Minnesota Pollution Control Agency.

Minnesota Pollution Control Agency (MPCA). (2013). *Nitrogen in Minnesota surface waters: Conditions, trends, sources, and reductions*. (Doc. wq-s6–26a, 510 pp.). St. Paul, MN: Minnesota Pollution Control Agency.

Mitsch, W. J., Day, J. W., Zhang, L., & Lane, R. R. (2005). Nitrate-nitrogen retention in wetlands in the Mississippi River Basin. *Ecological Engineering*, *24*(4), 267–278. https://doi.org/10.1016/j.ecoleng.2005.02.005

Mulholland, P. J., Helton, A. M., Poole, G. C., Hall, R. O., Hamilton, S. K., Peterson, B. J., et al. (2008). Stream denitrification across biomes and its response to anthropogenic nitrate loading. *Nature*, *452*(7184), 202–205. https://doi.org/10.1038/nature06686

Park, C. C. (1977). World-wide variations in hydraulic geometry exponents of stream channels: An analysis and some observations. *Journal of Hydrology*, *33*, 133–146. https://doi.org/10.1016/0022-1694(77)90103-2

Payne, E. G. I., Fletcher, T. D., Russell, D. G., Grace, M. R., Cavagnaro, T. R., Evrard, V., et al. (2014). Temporary storage or permanent removal? The division of nitrogen between biotic assimilation and denitrification in stormwater biofiltration systems. *PLoS ONE*, *9*(3), e90890. https://doi.org/10.1371/journal.pone.0090890

Perry, W., Broers, A., El-Baz, F., Harris, W., Healy, B., Hillis, W. D., et al. (2008). *Grand challenges for engineering* (52 pp.). Washington, DC: National Academy of Engineering of the National Academies.

Pinay, G., Peiffer, S., De Dreuzy, J. R., Krause, S., Hannah, D. M., Fleckenstein, J. H., et al. (2015). Upscaling nitrogen removal capacity from local hotspots to low stream orders' drainage basins. *Ecosystems*, *18*(6), 1101–1120. https://doi.org/10.1007/s10021-015-9878-5

Powers, D. M. W. (2011). Evaluation: From precision, recall and F-measure to ROC, informedness, markedness and correlation. *Journal of Machine Learning Technologies*, *2*(1), 37–63.

Robertson, D. M., & Saad, D. A. (2014). SPARROW models used to understand nutrient sources in the Mississippi/Atchafalaya River Basin. *Journal of Environment Quality*, *42*(5), 1422–1440. https://doi.org/10.2134/jeq2013.02.0066

Rockström, J., Steffen, W., Noone, K., Persson, A., Chapin, F. S., 3rd, Lambin, E. F., et al. (2009). A safe operating space for humanity. *Nature*, *461*, 472–475. https://doi.org/10.1038/461472a

Rodriguez-Iturbe, I., & Rinaldo, A. (1997). *Fractal river basins: Chance and self-organization* (564 pp.). New York, NY: Cambridge University Press.

Royer, T. V., David, M. B., & Gentry, L. E. (2006). Timing of riverine export of nitrate and phosphorus from agricultural watersheds in Illinois: Implications for reducing nutrient loading to the Mississippi River. *Environmental Science and Technology*, *40*(13), 4126–4131. https://doi.org/10.1021/es052573n

Schilling, K. E., Jones, C. S., Seeman, A., Bader, E., & Filipiak, J. (2012). Nitrate-nitrogen patterns in engineered catchments in the upper Mississippi River Basin. *Ecological Engineering*, *42*, 1–9. https://doi.org/10.1016/j.ecoleng.2012.01.026

Seitzinger, S., Harrison, J. A., Bohlke, J. K., Bouwman, A. F., Lowrance, R., Peterson, B., et al. (2006). Denitrification across landscapes and waterscapes: A synthesis. *Ecological Applications*, *16*(6), 2064–2090. https://doi.org/10.1890/1051-0761(2006)016[2064:DALAWA]2.0.CO;2

Seitzinger, S. P. (1988). Denitrification in freshwater and coastal marine ecosystems; Ecological and geochemical significance. *Limnology and Oceanography*, *33*(4), Part 2, 702–724. https://doi.org/10.4319/lo.1988.33.4part2.0702

Seitzinger, S. P., Styles, R. V., Boyer, E. W., Alexander, R. B., Billen, G., Howarth, R. W., et al. (2002). Nitrogen retention in rivers: Model development and application to watersheds in the northeastern USA. *Biogeochemistry*, *57*(1), 199–237. https://doi.org/10.1023/A:1015745629794

Smith, R. A., Schwarz, G. E., & Alexander, R. B. (1997). Regional interpretation of water-quality monitoring data. *Water Resources Research*, *33*(12), 2781–2798. https://doi.org/10.1029/97WR02171

Soranno, P. A., Webster, K. E., Riera, J. L., Kratz, T. K., Baron, J. S., Bukaveckas, P. A., et al. (1999). Spatial variation among lakes within landscapes: Ecological organization along lake chains. *Ecosystems*, *2*(5), 395–410. https://doi.org/10.1007/s100219900089

Stelzer, R. S., Scott, J. T., & Bartsch, L. A. (2015). Buried particulate organic carbon stimulates denitrification and nitrate retention in stream sediments at the groundwater–surface water interface. *Freshwater Science*, *34*(1), 161–171. https://doi.org/10.1086/678249

Stubbins, A. (2016). A carbon for every nitrogen. *Proceedings of the National Academy of Sciences of the United States of America*, *113*(38), 201612995. https://doi.org/10.1073/pnas.1612995113

Tank, J. L., Rosi-Marshall, E. J., Baker, M. A., & Hall, R. O. (2008). Are rivers just big streams? A pulse method to quantify nitrogen demand in a large river. *Ecology*, *89*(10), 2935–2945. https://doi.org/10.1890/07-1315.1

Taylor, P. G., & Townsend, A. R. (2010). Stoichiometric control of organic carbon–nitrate relationships from soils to the sea. *Nature*, *464*(7292), 1178–1181. https://doi.org/10.1038/nature08985

Thiere, G., Stadmark, J., & Weisner, S. E. B. (2011). Nitrogen retention versus methane emission: Environmental benefits and risks of large-scale wetland creation. *Ecological Engineering*, *37*(1), 6–15. https://doi.org/10.1016/j.ecoleng.2009.02.002

Turner, R. E., Rabalais, N. N., & Justic, D. (2008). Gulf of Mexico hypoxia: Alternate states and a legacy. *Environmental Science & Technology*, *42*(7), 2323–2327. https://doi.org/10.1021/es071617k

U.S. Geological Survey (USGS). (2016). *USGS 05320500 Le Sueur River near Rapidan, MN*. Retrieved from http://waterdata.usgs.gov/nwis/uv?site_no=05320500

Vachon, D., Prairie, Y. T., Guillemette, F., & del Giorgio, P. A. (2017). Modeling allochthonous dissolved organic carbon mineralization under variable hydrologic regimes in boreal lakes. *Ecosystems*, *20*(4), 781–795. https://doi.org/10.1007/s10021-016-0057-0

Vymazal, J. (2007). Removal of nutrients in various types of constructed wetlands. *Science of the Total Environment*, *380*(1–3), 48–65. https://doi.org/10.1016/j.scitotenv.2006.09.014

Wilson, H. F., & Xenopoulos, M. A. (2008). Effects of agricultural land use on the composition of fluvial dissolved organic matter. *Nature Geoscience*, *2*(1), 37–41. https://doi.org/10.1038/ngeo391

Wollheim, W. M., Harms, T. K., Peterson, B. J., Morkeski, K., Hopkinson, C. S., Stewart, R. J., et al. (2014). Nitrate uptake dynamics of surface transient storage in stream channels and fluvial wetlands. *Biogeochemistry*, *120*(1–3), 239–257. https://doi.org/10.1007/s10533-014-9993-y

Wollheim, W. M., Peterson, B. J., Thomas, S. M., Hopkinson, C. H., & Vörösmarty, C. J. (2008a). Dynamics of N removal over annual time periods in a suburban river network. *Journal of Geophysical Research*, *113*, G03038. https://doi.org/10.1029/2007JG000660

Wollheim, W. M., Stewart, R. J., Aiken, G. R., Butler, K. D., Morse, N. B., & Salisbury, J. (2015). Removal of terrestrial DOC in aquatic ecosystems of a temperate river network. *Geophysical Research Letters*, *42*, 6671–6679. https://doi.org/10.1002/2015GL064647

Wollheim, W. M., Vörösmarty, C. J., Bouwman, A. F., Green, P., Harrison, J., Linder, E., et al. (2008b). Global N removal by freshwater aquatic systems using a spatially distributed, within-basin approach. *Global Biogeochemical Cycles*, *22*, GB2026. https://doi.org/10.1029/2007GB002963

Wollheim, W. M., Vörösmarty, C. J., Peterson, B. J., Seitzinger, S. P., & Hopkinson, C. S. (2006). Relationship between river size and nutrient removal. *Geophysical Research Letters*, *33*, L06410. https://doi.org/10.1029/2006GL025845

Zarnetske, J. P., Haggerty, R., Wondzell, S. M., & Baker, M. A. (2011). Labile dissolved organic carbon supply limits hyporheic denitrification. *Journal of Geophysical Research*, *116*, G04036. https://doi.org/10.1029/2011JG001730